

New Journal of Chemistry

Supporting Information

In situ preparation of ferric polymeric aluminum chloride-silica gel nanocatalyst by mechanical grinding and its solid-phase catalytic behavior in organic synthesis

Yuwang Liang ^{a,‡}, Gang Wang ^{a,‡}, Xiang Li ^a, Qiuping Zhang ^a, Haijuan Zhan ^{a,*}, Shuxian Bi ^a, Zhiqiang Wu ^b, Wanyi Liu ^{a,*}

^a State Key Laboratory of High-efficiency Utilization of Coal and Green Chemical Engineering, National Demonstration Center for Experimental Chemistry Education, College of Chemistry and Chemical Engineering, Ningxia University, Yinchuan 750021, P. R. China.

^b College of Chemistry and Chemical Engineering, Ningxia Normal university, Guyuan 756000, P. R. China.

Corresponding author:

Wanyi Liu, State Key Laboratory of High-efficiency Utilization of Coal and Green Chemical Engineering, College of Chemistry and Chemical Engineering, Ningxia University, Yinchuan 750021, People's Republic of China. Email: liuwy@nxu.edu.cn.

1 General experimental condition

1.1 Chemicals and instruments

All reagents are more than 98% pure and the solvent is A.R. It is used directly after purchase. Poly Aluminum Ferric Chloride (PAFC) is reddish brown powder, the content of alumina is about 30%, the content of Iron oxide is about 5%, in accordance with the GB15892-2003 standard, China henan kechuang purification materials co, LTD. Scanning electron microscope (SEM) image recorded on the Hitachi S4800. The morphology of the materials was obtained on JEOL JEM-2010F High Resolution Transmission Electron Microscope (HRTEM). FTIR spectral analysis by Bruker TENSOR 27Two03040404. ^1H and ^{13}C NMR were obtained by Bruker 400 MHz spectrometer. The X-ray photoemission (XPS) spectra were performed at room temperature using a Thermo ESCALAB 250xi hemispherical electron energy analyzer.

1.2 Typical procedure for the synthesis of 3-alkylindole derivatives

Put polyaluminum ferric chloride (0.05g), 300-400 mesh silica gel (0.2g) in a mortar, solid-phase grinding for 20 minutes at room temperature, prepare PLASC catalyst in situ, and add indole (1mmol), styrene oxide (1.5mmol), continue solid-phase grinding at room temperature, and TLC monitors the progress of the reaction. After the completion of the reaction, the reaction mixture was washed and extracted with ethyl acetate (3×10 mL), the residue solid after extraction was the catalyst, and it was dried in a vacuum oven at 30°C for 30 minutes (It can be used for the next batch reaction). The extracted organic phase contains the reaction product and unreacted substrate, the extraction solvent ethyl acetate is recovered by distillation, and the crude product is purified by column chromatography (petroleum ether: ethyl acetate 7:3), finally, the structure of the product is determined by NMR.

1.3 Typical procedure for the synthesis of Quinoxalines

Put polyaluminum ferric chloride (0.01g), 300-400 mesh silica gel (0.05g) in a mortar, solid-phase grinding for 20 minutes at room temperature, prepare PLASC catalyst in situ, and add α -dicarbonyls (1 mmol), 1,2-diamines (1mmol), continue solid-phase grinding at room temperature, and TLC monitors the progress of the reaction.

After the completion of the reaction, the reaction mixture was washed and extracted with ethyl acetate (3×10 mL), the residue solid after extraction was the catalyst, and it was dried in a vacuum oven at 30°C for 30 minutes (It can be used for the next batch reaction). The extracted organic phase contains the reaction product and unreacted substrate, the extraction solvent ethyl acetate is recovered by distillation, and the crude product is purified by column chromatography (petroleum ether: ethyl acetate 10:1), finally, the structure of the product is determined by NMR.

1.4 Typical procedure for the synthesis of benzimidazole derivatives

Put polyaluminum ferric chloride (0.05g), 300-400 mesh silica gel (0.2g) in a mortar, solid-phase grinding for 20 minutes at room temperature, prepare PLASC catalyst in situ, and add benzaldehyde (1 mmol), 1,2-diamines (1mmol), continue solid-phase grinding at room temperature, and TLC monitors the progress of the reaction. After the completion of the reaction, the reaction mixture was washed and extracted with ethyl acetate (3×10 mL), the residue solid after extraction was the catalyst, and it was dried in a vacuum oven at 30°C for 30 minutes (It can be used for the next batch reaction). The extracted organic phase contains the reaction product and unreacted substrate, the extraction solvent ethyl acetate is recovered by distillation, and the crude product is purified by column chromatography (petroleum ether: ethyl acetate 2:1), finally, the structure of the product is determined by NMR.

1.4 Typical procedure for the synthesis of β -amino alcohol derivatives

Put polyaluminum ferric chloride (0.05g), 300-400 mesh silica gel (0.2g) in a mortar, solid-phase grinding for 20 minutes at room temperature, prepare PLASC catalyst in situ, and add aniline (1 mmol), styrene oxide (1mmol), continue solid-phase grinding at room temperature, and TLC monitors the progress of the reaction. After the completion of the reaction, the reaction mixture was washed and extracted with ethyl acetate (3×10 mL), the residue solid after extraction was the catalyst, and it was dried in a vacuum oven at 30°C for 30 minutes (It can be used for the next batch reaction). The extracted organic phase contains the reaction product and unreacted substrate, the extraction solvent ethyl acetate is recovered by distillation, and the crude product is purified by column chromatography (petroleum ether: ethyl acetate 5:1), finally, the

structure of the product is determined by NMR.

2. The characterization results and experimental data

Table S1. Condition optimization of synthesis reaction of 3-alkylinole by PLASC catalysts

Entry	Main catalyst/g	Co-catalyst Silica gel/g	Main product 3 yields ^a
1	/	/	N.R ^b
2	/	0.5	N.R
3	PAFC (0.05)	/	29
4	PAFC (0.02)	0.5	56
5	PAFC (0.05)	0.5	74
6	PAFC (0.10)	0.5	73
7	PAFC (0.05)	0.3	73
8	PAFC (0.05)	0.2	74
9	PAFC (0.05)	0.1	41
10 ^c	PAFC (0.05)	0.2	57
11 ^d	PAFC (0.05)	0.2	52
12 ^e	PAFC (0.05)	0.2	75
13 ^f	PAFC (0.05)	/	40
14	PAC (0.05)	/	25
15	PAC (0.05)	0.2	49
16	AlCl ₃ ·6H ₂ O (0.1mmol)	0.2	24
17	FeCl ₃ ·6H ₂ O (0.1mmol)	0.2	22
18	AlCl ₃ ·6H ₂ O (0.1mmol) +SDS	0.2	47
19	FeCl ₃ ·6H ₂ O (0.1mmol) +SDS	0.2	31
20	PAFC (0.05) +SDS	0.2	61
21	PAC (0.05) +SDS	0.2	35
22 ¹	In(NO) ₃ ·3H ₂ O (0.1mmol)	0.2	70
23 ²	50%wtHBF ₄ aqueous solution 0.3g	0.2	72

Reaction conditions: Put polyaluminum ferric chloride and 300-400 mesh silica gel in a mortar, solid-phase grinding for 20 minutes at room temperature, then add indole (1 mmol) and styrene oxide (1.2 mmol), and grind for 30 minutes at room temperature.

^a Isolated yields.

^b No product is formed.

^c The feeding amount is 1 mmol of indole and 1 mmol of styrene oxide.

^d The feeding amount is 1.2 mmol of indole and 1 mmol of styrene oxide.

^e Solvent is CH₂Cl₂.

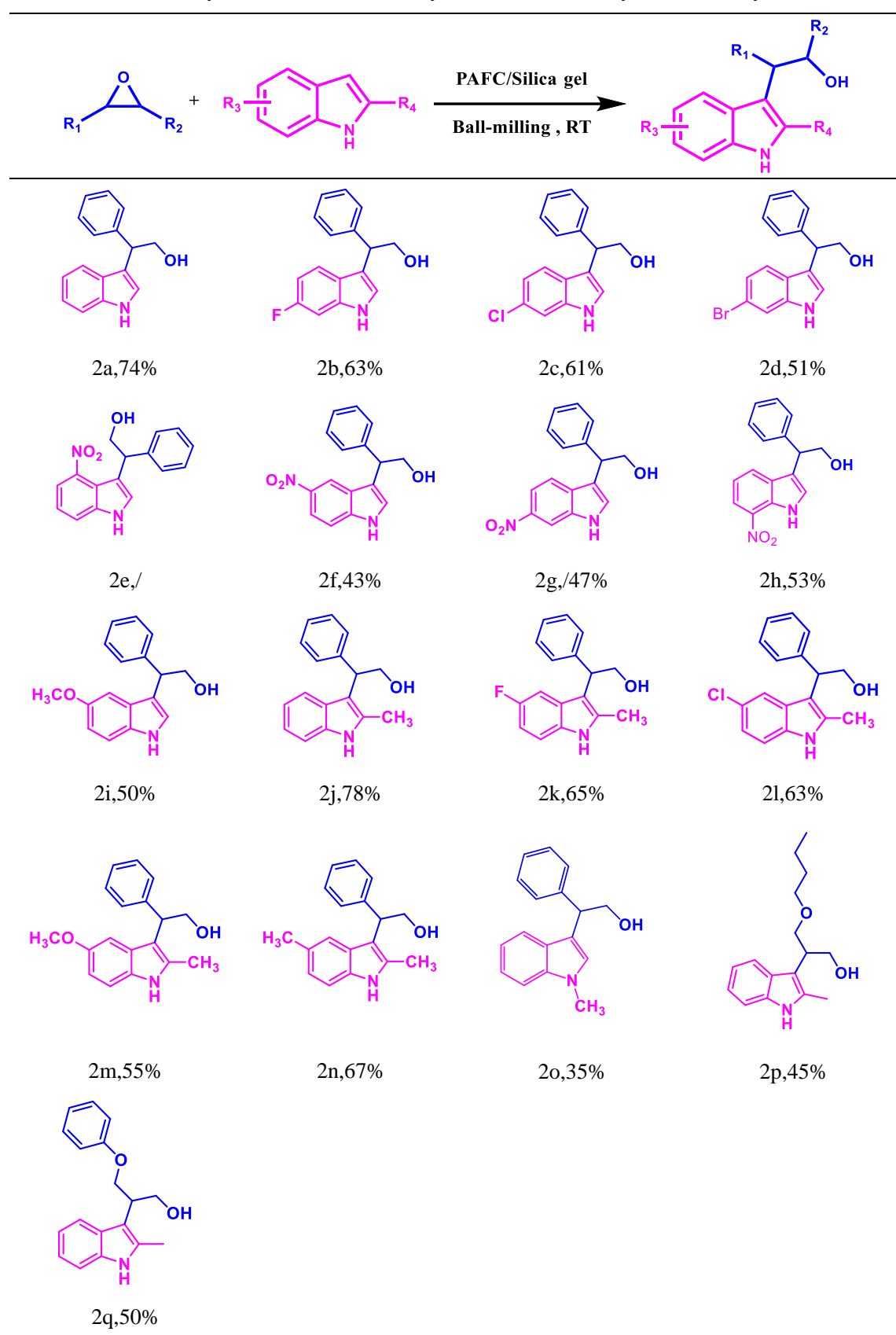
^f Solvent is CH₂Cl₂ and no co-catalyst silica gel are added, and the reaction time is 3h.

Table S2. Amplification response

Reaction type	Magnification	Yields (1mmol/10μmol) %
Synthesis reaction of 3-alkylindole derivatives	10	74/72
Synthesis reaction of β -amino alcohol derivatives	10	90/87
Synthesis reaction of benzimidazole derivatives	10	91/90
Synthesis reaction of quinoxaline derivatives	10	99/99

The reaction conditions are the same as the small test conditions

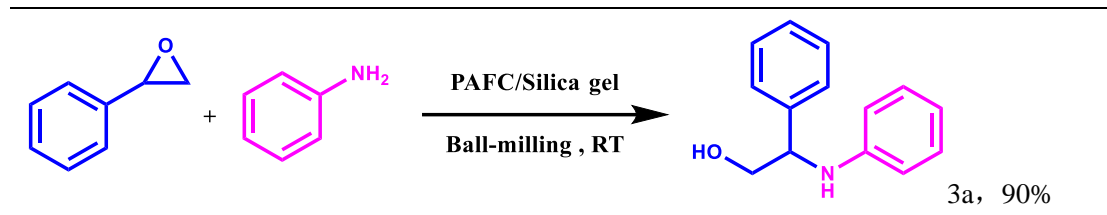
Table S3. Synthesis reaction of 3-alkylindole derivatives by PLASC catalysts



Reaction conditions: polyaluminum ferric chloride (0.05g), 300-400 mesh silica gel (0.2g) in a mortar, solid-phase grinding at room temperature for 20 minutes, then add indole derivative (1mmol), styrene oxide Derivative (1.2mmol), grind at room temperature for 30min.

Isolated yields.

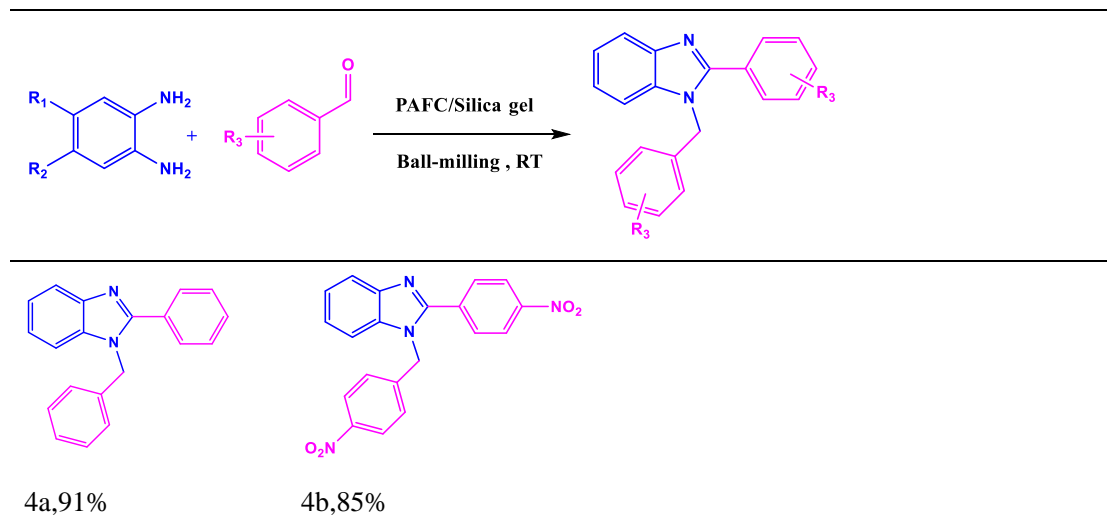
Table S4. Synthesis reaction of β -amino alcohol derivatives by PLASC catalysts



Reaction conditions: polyaluminum ferric chloride (0.05g), 300-400 mesh silica gel (0.2g) in a mortar, solid-phase grinding at room temperature for 20 minutes, then add aniline (1mmol), styrene oxide (1.2mmol)), grind for 30min at room temperature.

Isolated yields.

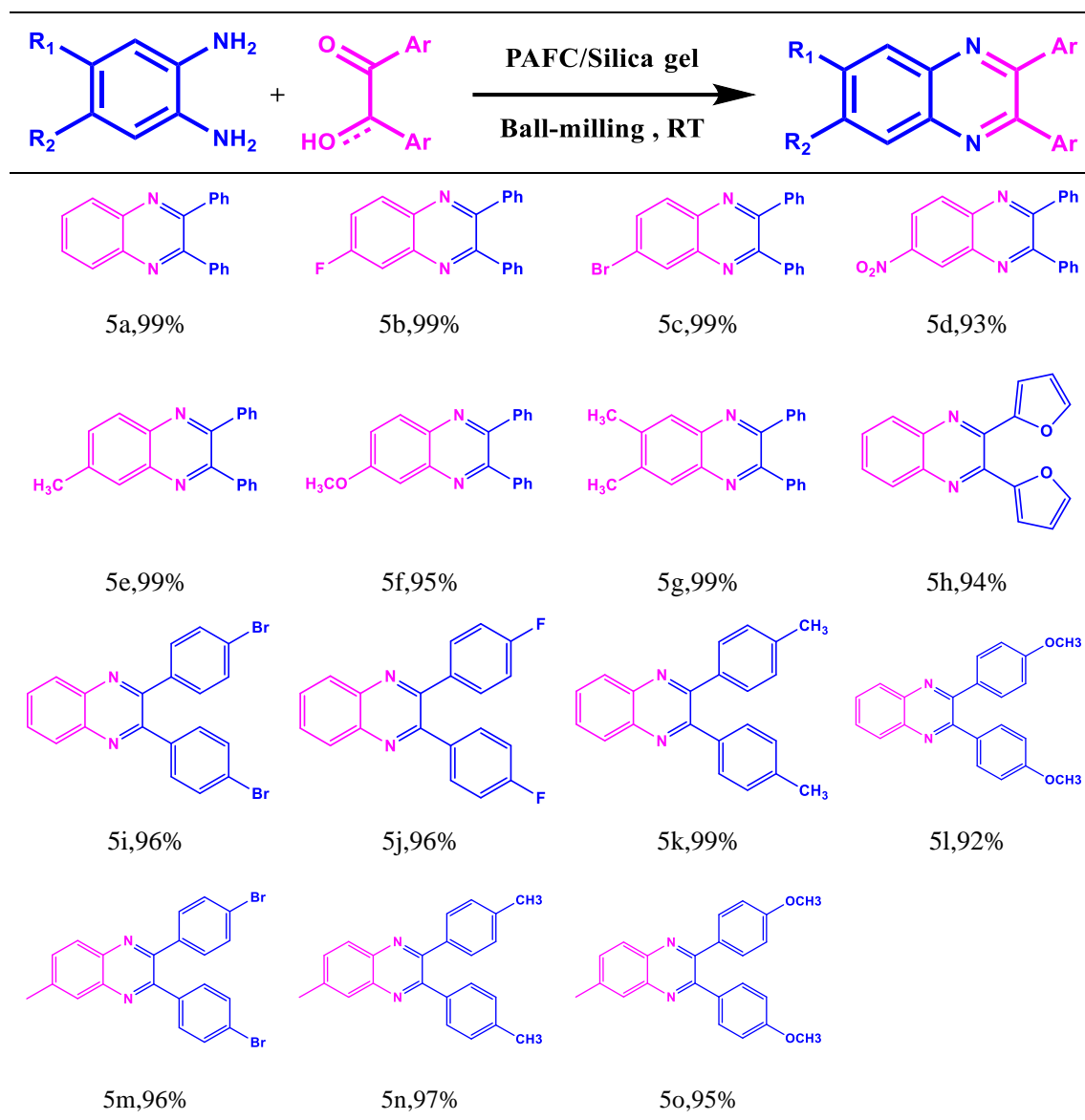
Table S5. Synthesis reaction of benzimidazole derivatives by PLASC catalysts



Reaction conditions: polyaluminum ferric chloride (0.05g), 300-400 mesh silica gel (0.2g) in a mortar, solid-phase grinding at room temperature for 20 minutes, then add o-phenylenediamine derivative (1mmol), benzaldehyde derived (2 mmol), grind at room temperature for 20 min.

Isolated yields.

Table S6. Synthesis reaction of quinoxaline derivatives by PLASC catalysts



Reaction conditions: polyaluminum ferric chloride (0.01g), 300-400 mesh silica gel (0.04g) in a mortar, solid-phase grinding at room temperature for 20 minutes, then add o-phenylenediamine derivative (1mmol), benzil Derivative (1 mmol), grind at room temperature for 5 min.

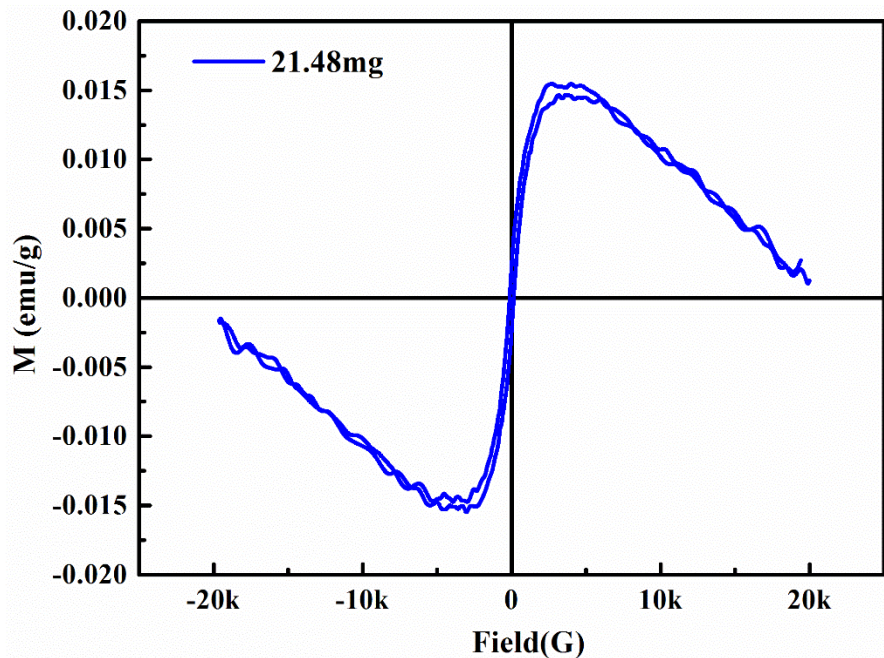
Isolated yields.

Table S7 BET and pore size of the catalysts

	BET /(m ² /g)	Desorption average pore diameter (4V/A by BET)/(nm)
Silica gel	343.8321	10.9328 nm
PLASC after useing one time	248.3609	8.7548
PLASC after using ten times	287.6113	7.8495

Table S8 Zeta potential of the catalysts

	1	2	3	Average
Silica gel	-0.6324	-0.6496	-0.5772	-0.6197
PAFC	+0.4384	+0.4628	+0.4086	+0.4366
PLASC after useing one time	-0.1690	-0.1928	-0.1574	-0.1730
PLASC after useing ten times	-0.9367	-1.1139	-0.8816	-0.9774



FigureS1. VSM of PLASC catalysts

The magnetic test results for the PLASC catalyst are shown in Figure S2. The results show that the inclusion of ferric polymeric aluminium chloride does give the composite catalyst some magnetic properties, but the magnetic properties are very weak, PLASC catalysts showed a saturation magnetization (M_s) value of 0.0152 emu/g, and we do not believe that there is a significant correlation between the magnetic properties and the catalytic effect of the catalyst. The iron in the polymeric aluminium chloride iron mainly adjusts the electronic structure in the composite, and the very small amount of Fe-O bonding improves the charge distribution of the composite, effectively promoting its electron transport and enhancing the catalytic activity of the composite catalyst.

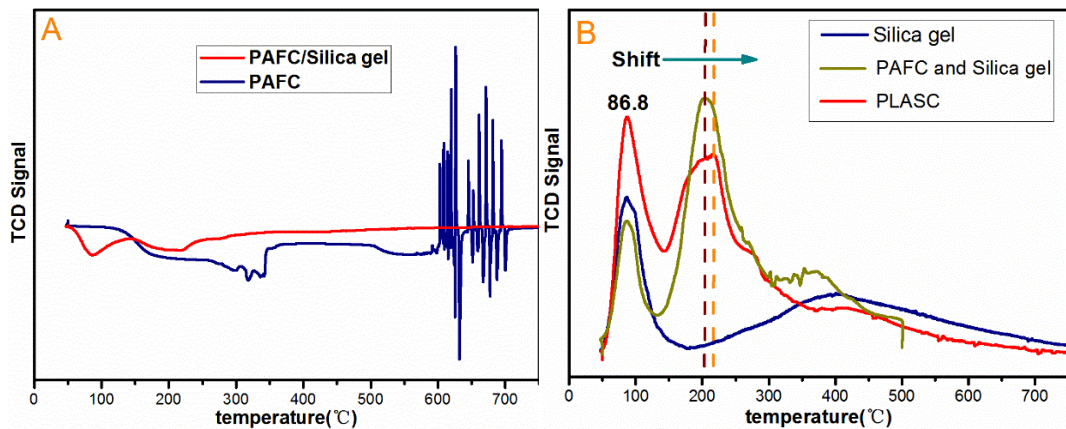


Figure S2. PLASC catalyst NH₃TPD

Figure S3. is PAFC and PLASC catalyst NH₃-TPD, B is silica gel, PAFC and silica gel physically mixed, PAFC/silica gel composite NH₃-TPD. Figure A shows that PAFC begins to decompose around 600°C, and the PLASC composite formed by PAFC and silica gel remains stable at 700°C after grinding. This is due to the Si-O-Al, Si-O- formed in-situ during the grinding process. The Fe bond is more stable than the original Al-O-Fe and Al-O-Al bonds. Figure B shows: Compared with silica gel and the physical mixture of PAFC and silica gel, after mechanical grinding of PAFC and silica gel, the physical adsorption peak around 90°C is obviously increased. Combined with the SEM image, it can be seen that this is due to the particle size of the material due to the grinding effect. Smaller, increased surface area, and looser material surface, which is also a manifestation of nanomaterials. The chemisorption peak near 200 °C shifts toward higher temperature, indicating that Si-O-Al and Si-O are formed in situ At the same time as the active bond sites of Fe, the acid sites of the catalyst are transformed into strong acid sites, which is one of the reasons why the catalytic activity of PLASC catalyst is stronger than that of PAFC itself.

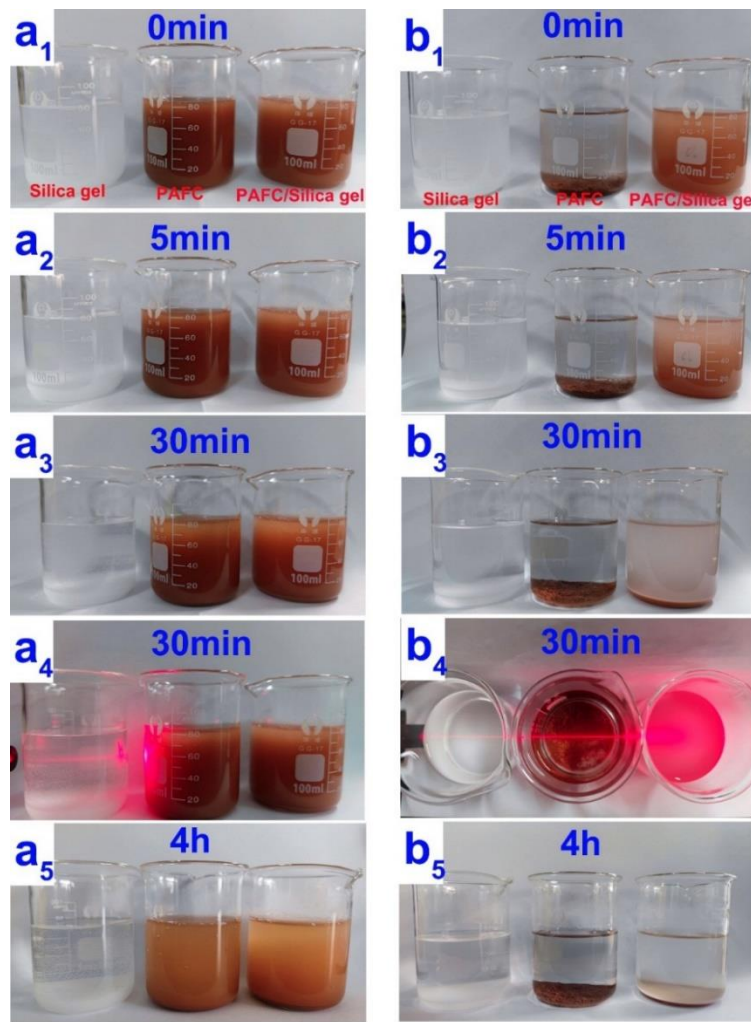


Figure S3. Morphological performance of materials in water and ethanol

a, b are the morphological performance of silica gel, PAFC, PLASC in water and ethanol, respectively. From a1 to a5, it can be seen that PAFC and PLASC form a turbid suspension after shaking in water, and the precipitation rate is very slow. The comparison is made after 4h, because of the $-\text{O}-\text{Si}-\text{O}-\text{Fe}-\text{O}-/\text{-O}-$ in PLASC $\text{Si}-\text{O}-\text{Al}-\text{O}-$ makes it more stable, and its precipitation rate is higher than that of PAFC alone. From b1 to b5, we can see that in ethanol, PAFC and PLASC are generally more stable than water, and the precipitation rate is higher. The laser test at 30 min in b4 shows that PAFC has Tyndall effect in ethanol due to its small part- The $-\text{Fe}-\text{O}-$, $-\text{Al}-\text{O}-$ bond reacts with ethanol to form a colloid, but the PAFC/silica gel composite under the same conditions does not show this phenomenon, which proves that the PLASC after grinding is more stable. As for its slightly turbidity, As shown by the finely divided silica gel after grinding.

Table S9. Comparison of E-factors in the synthesis of 3-alkylindole catalyzed by different catalysts

Reactant						
Entry	Indole/styrene oxide (mmol)	Catalyst dosage/reuse (times)	Solvent (ml)	Yield(%)	E factor	
1 ³	0.25/0.3	15mgMIL-101(Fe)/ 4	/	91	0.005	
2 ⁴	1/1	50mgMCM-41/5	/	80	0.055	
3 ⁵	1/1	2mmol[H-NMP]H ₂ PO ₄ /4 NMP]H ₂ PO ₄ /4	2mmol[H-NMP]H ₂ PO ₄ /4 NMP]H ₂ PO ₄ /4	85	1.289	
4 ⁶	1/1	0.5mmolNano MgO/5	/	70	0.025	
5 ⁷	1/1	10%molNano Fe ₃ O ₄ /2	/	76	0.065	
6 ⁸	1.2/1	0.5mL [bmim][OTf]/4	0.5mL [bmim][OTf]	85	0.751	
7 ¹	1/1	10%molInCl ₃ /0	2mlCH ₂ Cl ₂	85	13.786	
8 ⁹	1/1	10%molLiClO ₄ /0	2mlCH ₃ CN	85	8.153	
This work	1/1.2	250mgPLASC	/	75	0.146	

Table S10. Peak assignment of FT-IR of PLASC catalyst

Peak position (cm ⁻¹)	Peak attribution
3414	Physically adsorb the stretching vibration of water molecules
1635	Bending vibration of -OH
1090	Anti-symmetric stretching vibration of Si-O-Si
965	Bending vibration of Si-OH
802, 473	Symmetrical stretching vibration and bending vibration of Si-O
569	Bending vibration of Fe-O, Al-O
776	Stretching vibration of Fe-O, Al-O
975cm	Bending vibration of Fe-OH, Al-OH
1088, 1154	Anti-symmetric stretching vibration of Fe-O-Al, Al-O-A

Table S11. Comparison of the synthesis of quinoxaline derivatives in solvent-free, water, and

ethanol

Solvent (5ml)	catalyst (0.06g)	Yield ^a
	PLASC	99
/	PAFC	95
	PAC	89
	PLASC	92
Water	PAFC	83
	PAC	81
	PLASC	99
Ethanol	PAFC	99
	PAC	99

Reaction conditions: Put polyaluminum iron chloride (0.01g) and 300-400 mesh silica gel (0.04g) in a mortar, solid-phase grinding for 20 minutes at room temperature, then add o-phenylenediamine derivative (1mmol), benzene Acyl derivative (1 mmol), grind at room temperature for 5 min or add the catalyst, substrate, and solvent to the reaction tube and stir at room temperature for 30 min.

^aIsolated yields.

In view of the physical performance of the materials in different solvents, we explored the catalytic effects in their respective systems. The results are shown in Table S11. Under three conditions, such as solvent-free, water and ethanol, the catalytic effect of PAFC is generally higher than that of PAC, while PLASC The catalytic effect of PAFC is higher than that of PAFC alone. Obviously, the doping of Fe element improves the catalytic effect, and the catalytic performance of the new species after grinding is more prominent. At the same time, we observed that in terms of the final yield, the performance of solvent-free and ethanol-solvent conditions is significantly better than that of water-solvent. When ethanol is the solvent, the performance of various catalysts is more prominent than that under solvent-free. This may be due to ethanol in this

synthesis system. It's not surprising that PLASC in the solvent-free system can achieve the same effect as that in the ethanol system. This just illustrates the superior effect of PLASC catalyst in maintaining the output. At the same time, the use of organic solvents is avoided.

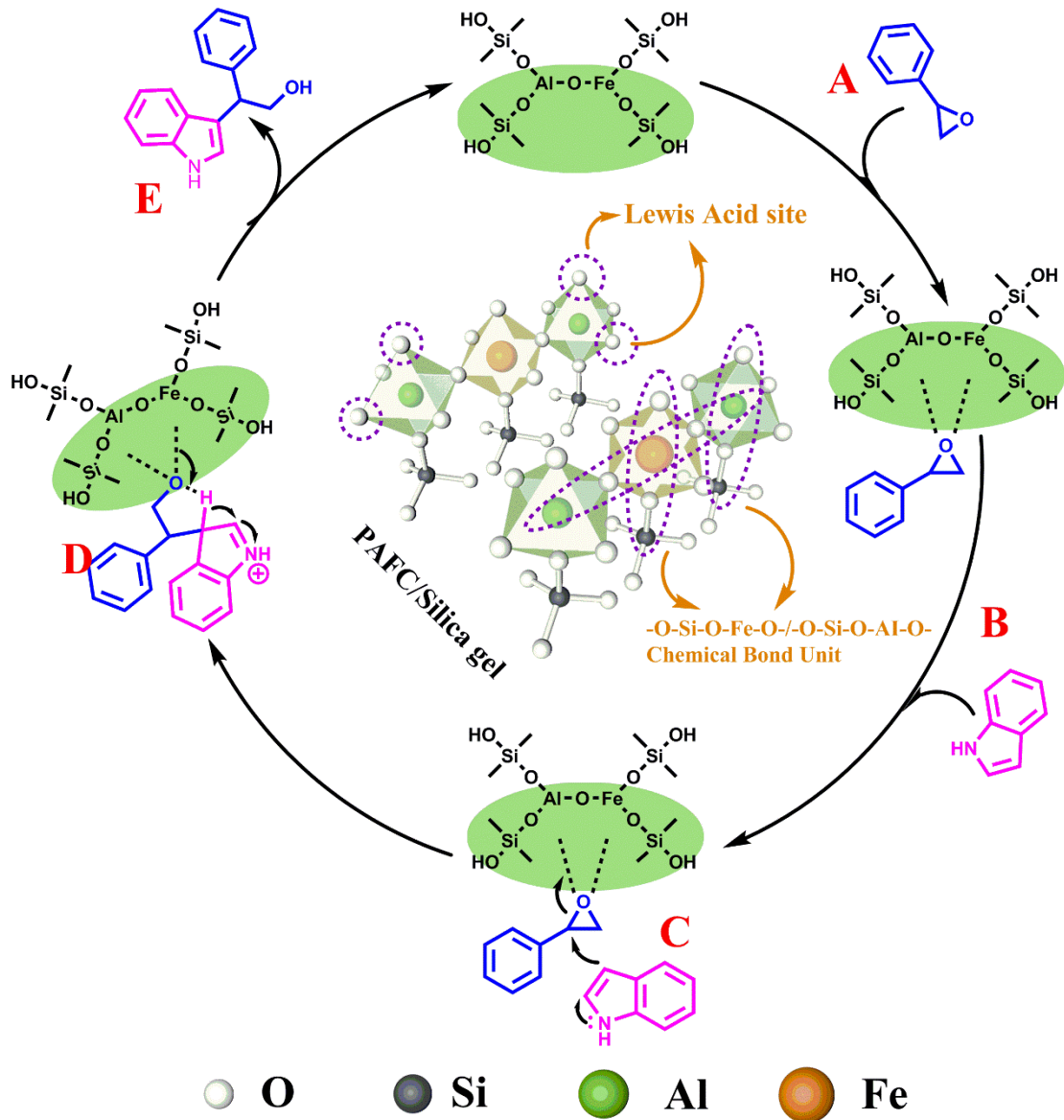
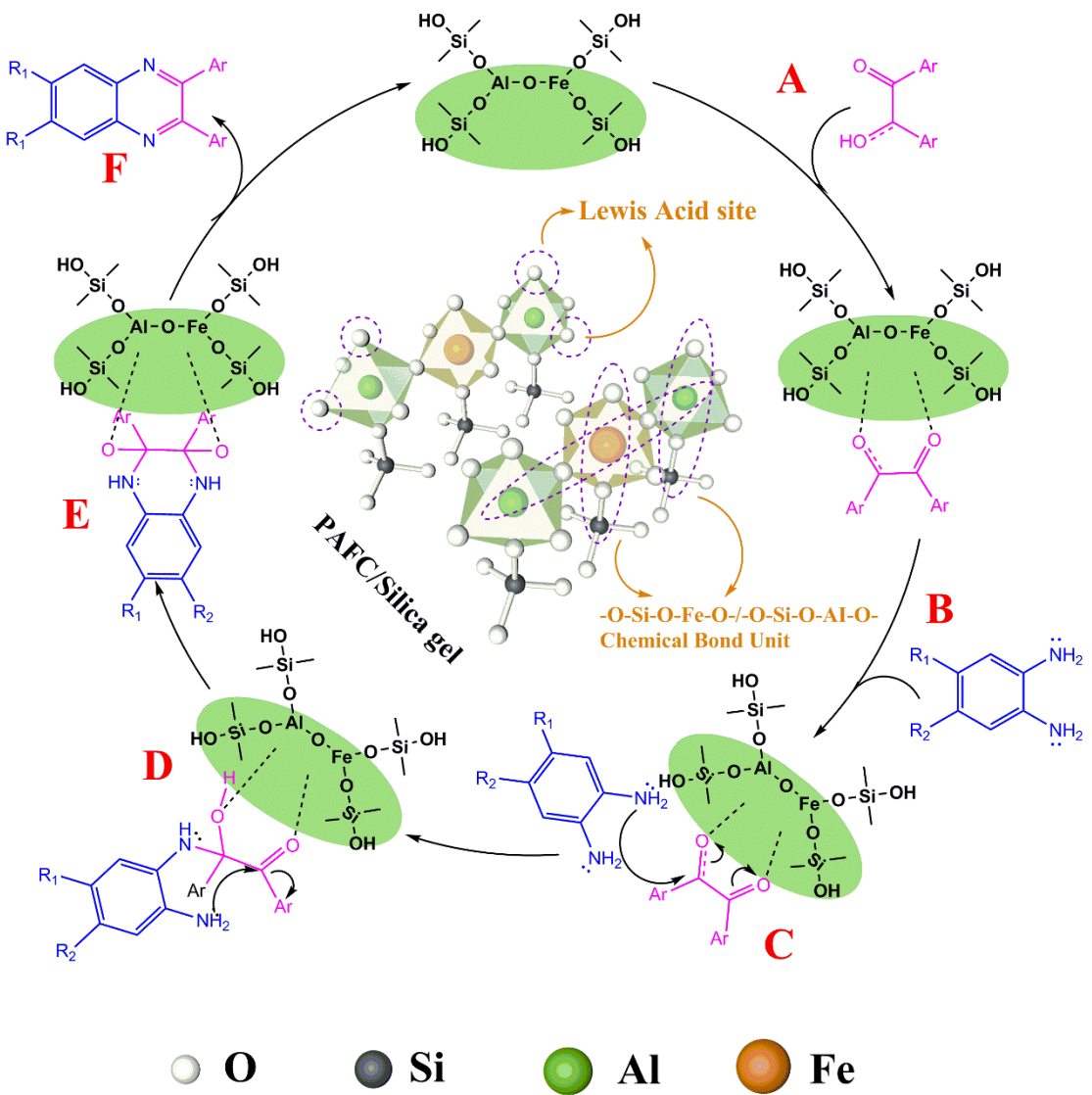


Figure S4. Mechanism of PLASC-catalyzed synthesis of 3-alkylindole derivatives

Based on conditional screening experiments and subsequent characterization and analysis of the morphology, FT-IR and XPS of the PAFC/silica gel composite catalyst, we found and confirmed the existence of new active bond ($-\text{O}-\text{Si}-\text{O}-\text{Fe}-\text{O}-$, $-\text{O}-\text{Al}-\text{O}-\text{Si}-\text{O}-$) sites generated *in situ* during the grinding of PAFC and silica gel. On this basis, the catalytic active centers of nanofibers formed by the active bonds are evenly distributed in the system so that the new polynuclear metal species has a richer electronic structure, and the overall catalytic performance is improved. we inferred the

catalytic mechanism of the catalytic system (taking the synthesis of 3-alkylindole derivatives as an example), and the results are shown in Figure S5. First of all, PAFC and silica gel form a fibrous nano-scale active bond (-O-Si-O-Fe-O-, -O-Al-O-Si-O-) on the surface of silica gel through intermolecular interaction and coordination under the action of mechanical force in the continuous grinding process. After adding the raw materials in the one-pot cooking method, compared with the PAFC alone, the catalytic bond positions in the new species are more diverse, and at the same time it brings a richer electric field, and it is easier to form coordination with the styrene oxide (A) oxygen. The electron cloud density around the oxygen atom increases and the electronegativity increases. The two carbon atoms connected to the oxygen are positively charged. Due to the influence of the benzene ring, the carbon atom at the benzyl position is more positively charged, and at the same time indole (B) The activation is completed by charge transfer at the 3 position, as an electrophile, it preferentially attacks the more positively charged benzyl carbon. The epoxy styrene carbon-oxygen bond is broken and added to the indole 3-position, after which the catalyst is removed by reduction and elimination. , The reaction is complete. (For the rest of the reaction mechanism, please refer to attached figures S6-S8.)



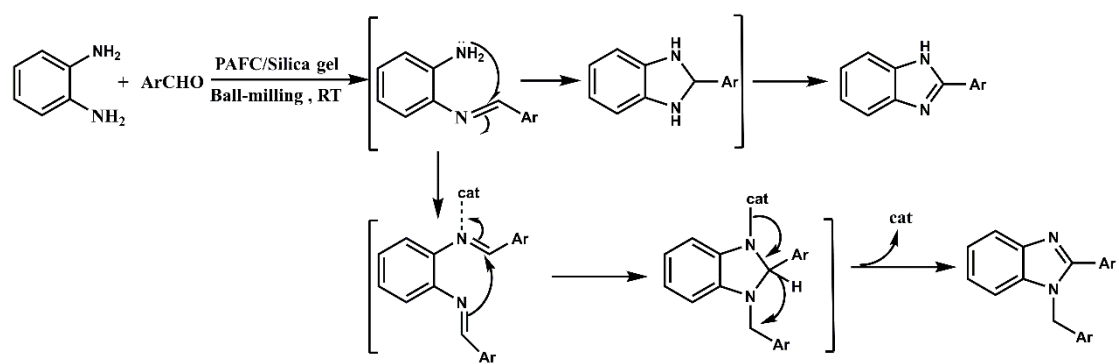


Figure S6. Mechanism of PLASC Catalyzed Synthesis of Benzodiazole Derivatives

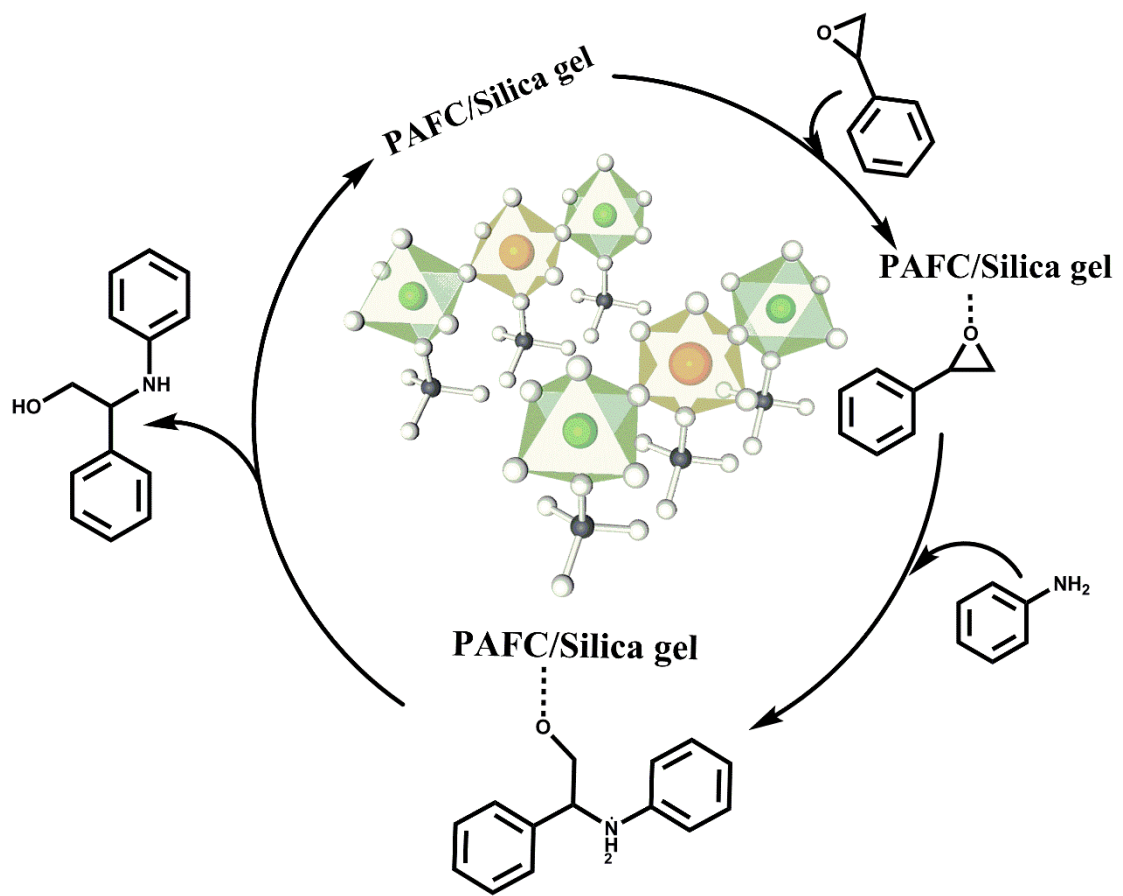


Figure S7. Mechanism of PLASC Catalyzed Synthesis of β -Amino Alcohol Derivatives

3. Characterization data of the products:



2-(1H-indol-3-yl)-2-phenylethan-1-ol (Table S2, 2a): Brown-red solid, 74%. ^1H NMR (400 MHz, CDCl_3) δ 8.10 (s, 1H), 7.42 (d, $J = 7.7$ Hz, 1H), 7.28 (s, 5H), 7.23 – 7.11 (m, 2H), 7.02 (d, $J = 7.7$ Hz, 1H), 6.96 (d, $J = 5.1$ Hz, 1H), 4.42 (t, $J = 7.2$ Hz, 1H), 4.23 – 4.07 (m, 2H). ^{13}C NMR (100 MHz, CDCl_3) δ 141.75, 136.51, 128.66, 128.37, 127.04, 126.79, 122.28, 122.03, 119.55, 119.39, 115.89, 111.30, 66.45, 45.65. (known compound⁵)



2-(6-fluoro-1H-indol-3-yl)-2-phenylethan-1-ol (Table S2, 2b): Brown-red solid, 63%. ^1H NMR (400 MHz, CDCl_3) δ 8.19 (s, 1H), 7.28 (t, $J = 4.2$ Hz, 5H), 7.21 (q, $J = 4.4$ Hz, 1H), 7.03 – 6.92 (m, 2H), 6.77 (td, $J = 9.2, 2.3$ Hz, 1H), 4.39 (t, $J = 6.8$ Hz, 1H), 4.22 – 4.05 (m, 2H). ^{13}C NMR (100 MHz, CDCl_3) δ 141.45, 136.43, 136.31, 128.72, 128.29, 126.92, 123.60, 122.14, 122.11, 120.14, 120.04, 116.01, 108.43, 108.18, 97.64, 97.38, 66.41, 45.53. (known compound⁵)



2-(6-chloro-1H-indol-3-yl)-2-phenylethan-1-ol (Table S2, 2c): Brown-red solid, 61%. ^1H NMR (400 MHz, CDCl_3) δ 8.17 (s, 1H), 7.30 (d, $J = 4.4$ Hz, 5H), 7.25 – 7.20 (m, 1H), 7.06 – 6.96 (m, 2H), 6.78 (td, $J = 9.2, 2.3$ Hz, 1H), 4.41 (t, $J = 6.8$ Hz, 1H), 4.23 – 4.06 (m, 2H). ^{13}C NMR (100 MHz, CDCl_3) δ 141.41, 136.43, 136.31, 128.72, 128.28, 126.92, 123.59, 122.11, 122.07, 120.16, 120.06, 116.06, 108.45, 108.20, 97.62, 97.37, 66.42, 45.53. (known compound⁵)



2-(6-bromo-1H-indol-3-yl)-2-phenylethan-1-ol (Table S2, 2d): Brown-red solid, 51%. ^1H NMR (400 MHz, CDCl_3) δ 8.27 (s, 1H), 7.48 – 7.15 (m, 7H), 7.07 (d, $J = 8.9$ Hz, 1H), 6.89 (s, 1H), 4.33 (t, $J = 6.7$ Hz, 1H), 4.15 – 3.99 (m, 2H). ^{13}C NMR (100 MHz, CDCl_3) δ 141.43, 137.24, 128.74, 128.30, 126.95, 125.93, 122.73, 122.61, 120.62, 116.05, 115.74, 114.22, 66.37, 45.44. (known compound⁵)



2-(5-nitro-1H-indol-3-yl)-2-phenylethan-1-ol (Table S2, 2f): yellow solid, 43%. ^1H NMR (400 MHz, DMSO) δ 11.79 – 11.66 (m, 1H), 8.30 (d, J = 2.3 Hz, 1H), 7.95 (dd, J = 9.0, 2.3 Hz, 1H), 7.56 (d, J = 2.3 Hz, 1H), 7.51 (d, J = 9.0 Hz, 1H), 7.37 – 7.33 (m, 2H), 7.28 (t, J = 7.5 Hz, 2H), 7.23 – 7.13 (m, 1H), 4.88 (t, J = 5.3 Hz, 1H), 4.40 (t, J = 6.9 Hz, 1H), 4.00 (dd, J = 32.8, 12.3, 5.9, 4.3 Hz, 2H). ^{13}C NMR (100 MHz, DMSO) δ 143.48, 140.55, 139.81, 128.67, 128.64, 126.83, 126.78, 126.60, 119.29, 116.86, 116.31, 112.27, 65.70, 45.36. (known compound³)



2-(6-nitro-1H-indol-3-yl)-2-phenylethan-1-ol (Table S2, 2g): yellow solid, 47%. ^1H NMR (400 MHz, DMSO-*d*₆) δ 11.72 (d, J = 2.5 Hz, 1H), 8.30 (d, J = 2.1 Hz, 1H), 7.83 – 7.73 (m, 2H), 7.50 (d, J = 8.8 Hz, 1H), 7.34 – 7.30 (m, 2H), 7.26 (dd, J = 8.4, 6.8 Hz, 2H), 7.19 – 7.14 (m, 1H), 4.87 (t, J = 5.3 Hz, 1H), 4.35 (t, J = 7.0 Hz, 1H), 4.07 – 3.93 (m, 2H). ^{13}C NMR (100 MHz, DMSO) δ 143.56, 142.19, 134.93, 132.12, 130.08, 128.63, 128.60, 126.52, 119.31, 117.86, 113.94, 108.65, 65.54, 45.42. (known compound³)



2-(7-nitro-1H-indol-3-yl)-2-phenylethan-1-ol (Table S2, 2h): yellow solid, 53%. ^1H NMR (400 MHz, CDCl₃) δ 9.91 (s, 1H), 8.07 (dd, J = 8.1, 0.9 Hz, 1H), 7.68 (dt, J = 7.8, 0.8 Hz, 1H), 7.37 – 7.19 (m, 6H), 7.05 (t, J = 8.0 Hz, 1H), 4.46 (td, J = 6.6, 0.9 Hz, 1H), 4.26 – 4.08 (m, 2H). ^{13}C NMR (100 MHz, CDCl₃) δ 140.96, 132.87, 131.01, 129.77, 128.81, 128.27, 127.59, 127.14, 124.24, 119.45, 118.88, 117.76, 66.48, 45.28. (known compound³)



2-(5-methoxy-1H-indol-3-yl)-2-phenylethan-1-ol (Table S2, 2i): Brown-black solid, 50%. ^1H NMR (400 MHz, CDCl₃) δ 8.16 (s, 1H), 7.45 – 7.21 (m, 4H), 7.21 – 7.07 (m, 2H), 6.89 (d, J = 5.2 Hz, 1H), 6.86 – 6.76 (m, 2H), 4.36 (d, J = 6.9 Hz, 1H), 4.20 – 4.02 (m, 2H), 3.73 – 3.65 (m, 6H). ^{13}C NMR (100 MHz, CDCl₃) δ 153.86, 141.76, 131.74, 128.67, 128.38, 127.49, 126.78, 122.88, 115.50, 112.28, 112.04, 101.35, 66.40, 55.91, 45.65. (known compound⁵)



2-(2-methyl-1H-indol-3-yl)-2-phenylethan-1-ol (Table S2, 2j): Brown-black solid, 78%. ¹H NMR (400 MHz, CDCl₃) δ 7.94 (s, 1H), 7.42 (d, *J* = 7.6 Hz, 1H), 7.29 (d, *J* = 6.4 Hz, 2H), 7.19 (dt, *J* = 25.1, 9.6 Hz, 4H), 7.07 (t, *J* = 7.3 Hz, 1H), 6.99 (d, *J* = 7.5 Hz, 1H), 4.43 (q, *J* = 7.6 Hz, 1H), 4.27 (d, *J* = 7.7 Hz, 2H), 2.30 – 2.22 (m, 3H). ¹³C NMR (100 MHz, CDCl₃) δ 141.77, 135.52, 133.40, 128.49, 128.02, 127.74, 126.38, 121.12, 119.55, 119.25, 110.62, 110.05, 65.10, 45.14, 12.27. (known compound⁵)



2-(5-fluoro-2-methyl-1H-indol-3-yl)-2-phenylethan-1-ol (Table S2, 2k): Brown-black solid, 65%. ¹H NMR (400 MHz, CDCl₃) δ 8.06 (s, 1H), 7.33 – 7.24 (m, 4H), 7.18 (ddt, *J* = 8.5, 5.8, 2.1 Hz, 1H), 7.12 (dd, *J* = 8.8, 4.5 Hz, 1H), 7.06 (dd, *J* = 10.2, 2.5 Hz, 1H), 6.81 (td, *J* = 9.0, 2.5 Hz, 1H), 4.40 (dd, *J* = 8.8, 6.4 Hz, 1H), 4.33 – 4.19 (m, 2H), 2.32 (d, *J* = 1.3 Hz, 3H). ¹³C NMR (100 MHz, CDCl₃) δ 158.78, 156.46, 141.31, 135.28, 131.93, 128.56, 127.88, 126.51, 111.07, 110.97, 110.48, 110.44, 109.29, 109.03, 104.42, 104.18, 64.84, 44.90, 12.40, 12.39. (known compound³)



2-(5-chloro-2-methyl-1H-indol-3-yl)-2-phenylethan-1-ol (Table S2, 2l): Brown-black solid, 63%. ¹H NMR (400 MHz, CDCl₃) δ 8.08 (s, 1H), 7.39 (d, *J* = 1.9 Hz, 1H), 7.29 – 7.16 (m, 5H), 7.10 (d, *J* = 8.5 Hz, 1H), 7.01 (dd, *J* = 8.6, 2.0 Hz, 1H), 4.39 (dd, *J* = 8.8, 6.5 Hz, 1H), 4.32 – 4.19 (m, 2H), 2.28 (s, 3H). ¹³C NMR (100 MHz, CDCl₃) δ 141.24, 134.92, 133.79, 128.76, 128.59, 127.88, 126.56, 125.08, 121.28, 118.53, 111.53, 110.07, 64.93, 44.90, 12.35. (known compound³)



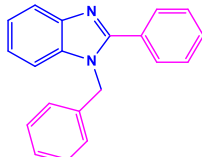
2-(5-methoxy-2-methyl-1H-indol-3-yl)-2-phenylethan-1-ol (Table S2, 2m): Brown-black solid, 55%. ¹H NMR (400 MHz, CDCl₃) δ 7.93 (s, 1H), 7.31 (d, *J* = 7.2 Hz, 2H), 7.24 (dt, *J* = 8.1, 6.9 Hz, 2H), 7.19 – 7.13 (m, 1H), 7.09 (d, *J* = 8.7 Hz, 1H), 6.87 (d, *J* = 2.4 Hz, 1H), 6.74 (dd, *J* = 8.7, 2.4 Hz, 1H), 4.42 (t, *J* = 7.6 Hz, 1H), 4.28 (d, *J* = 7.6 Hz, 2H), 3.71 (s, 3H), 2.27 (s, 3H). ¹³C NMR (100 MHz, CDCl₃) δ 153.76, 141.64, 134.26, 130.65, 128.46, 128.22, 127.99, 126.35, 111.13, 110.45, 109.82, 101.89, 64.91, 55.93, 55.89, 44.93, 12.39. (known compound³)



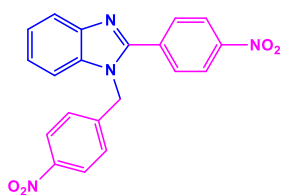
2-(2,5-dimethyl-1H-indol-3-yl)-2-phenylethan-1-ol (Table S2, 2n): Brown-black solid, 67%. ^1H NMR (400 MHz, CDCl_3) δ 7.84 (s, 1H), 7.37 – 7.30 (m, 2H), 7.26 (dt, J = 7.7, 5.7 Hz, 3H), 7.17 (dd, J = 12.1, 7.4 Hz, 2H), 6.97 – 6.90 (m, 1H), 4.46 (t, J = 7.7 Hz, 1H), 4.38 – 4.24 (m, 2H), 2.38 (s, 3H), 2.32 (s, 3H). ^{13}C NMR (100 MHz, CDCl_3) δ 141.77, 133.77, 133.53, 128.71, 128.44, 128.02, 128.00, 126.31, 122.65, 118.95, 110.23, 109.38, 65.11, 45.15, 21.70, 21.67, 12.35, 12.32. (known compound³)



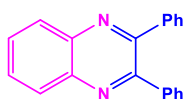
2-phenyl-2-(phenylamino)ethan-1-ol (Table S3, 3a): Yellowish brown solid, 90%. ^1H NMR (400 MHz, CDCl_3) δ 7.35 – 7.19 (m, 5H), 7.07 (q, J = 9.2, 8.6 Hz, 2H), 6.65 (q, J = 8.3 Hz, 1H), 6.53 (t, J = 9.0 Hz, 2H), 4.43 (p, J = 5.1 Hz, 1H), 3.86 (dt, J = 11.2, 5.6 Hz, 1H), 3.66 (td, J = 10.9, 6.8 Hz, 1H), 3.59 – 3.01 (m, 1H). ^{13}C NMR (100 MHz, CDCl_3) δ 147.29, 140.20, 129.24, 128.86, 127.65, 126.81, 117.96, 113.96, 67.34, 59.95. (known compound¹⁰)



1-benzyl-2-phenyl-1H-benzo[d]imidazole (Table S4, 4a): Brown solid, 91%. Brown-black solid, 74%. ^1H NMR (400 MHz, CDCl_3) δ 7.85 (d, J = 8.0 Hz, 1H), 7.70 – 7.65 (m, 2H), 7.47 – 7.40 (m, 3H), 7.31 (ddt, J = 8.2, 5.0, 3.0 Hz, 4H), 7.27 – 7.22 (m, 2H), 7.12 – 7.07 (m, 2H), 5.46 (s, 2H). ^{13}C NMR (100 MHz, CDCl_3) δ 153.97, 142.24, 136.13, 135.78, 130.24, 129.40, 129.27, 129.11, 128.88, 127.89, 125.99, 123.38, 123.07, 119.62, 110.76, 48.47. (known compound¹¹)

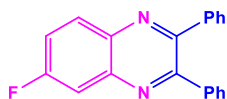


1-(4-nitrobenzyl)-2-(4-nitrophenyl)-1H-benzo[d]imidazole (Table S4, 4b): Crimson solid, 85%. ^1H NMR (400 MHz, DMSO) δ 8.39 – 8.31 (m, 2H), 8.21 – 8.13 (m, 2H), 8.05 – 7.98 (m, 2H), 7.82 (dd, J = 6.4, 2.8 Hz, 1H), 7.61 – 7.52 (m, 1H), 7.37 – 7.31 (m, 2H), 7.28 (d, J = 8.5 Hz, 2H), 5.85 (s, 2H). ^{13}C NMR (100 MHz, DMSO) δ 151.51, 148.45, 147.35, 144.80, 143.12, 136.54, 136.40, 130.80, 127.88, 124.49, 124.40, 124.18, 123.40, 120.29, 111.72, 47.66. (known compound¹¹)



2,3-Diphenyl-quinoxaline (Table S5, 5a): White solid, 99%. ^1H NMR (400 MHz, CDCl_3) δ 8.22 (dt, J = 6.8, 3.4 Hz, 1H), 7.77 (dt, J = 6.4, 3.4 Hz, 1H), 7.58 (dd, J = 7.7, 2.1 Hz, 2H), 7.44 – 7.32

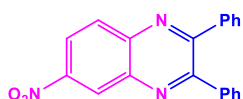
(m, 3H). ^{13}C NMR (100 MHz, CDCl_3) δ 153.47, 141.25, 139.11, 130.02, 129.92, 129.24, 128.87, 128.34. (known compound¹²)



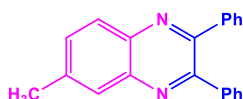
6-fluoro-2,3-diphenylquinoxaline (Table S5, 5b): White solid, 99%. ^1H NMR (400 MHz, CDCl_3) δ 8.19 (dd, $J = 9.2, 5.7$ Hz, 1H), 7.83 (dd, $J = 9.2, 2.8$ Hz, 1H), 7.59 – 7.52 (m, 5H), 7.37 (q, $J = 7.4, 6.9$ Hz, 6H). ^{13}C NMR (100 MHz, CDCl_3) δ 164.10, 161.60, 154.20, 152.85, 152.82, 142.01, 141.88, 138.81, 138.72, 138.43, 131.33, 131.23, 129.90, 129.84, 129.11, 128.94, 128.36, 120.50, 120.24, 112.77, 112.56. (known compound¹²)



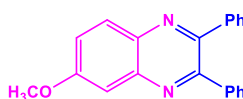
6-bromo-2,3-diphenylquinoxaline (Table S5, 5c): Light Yellow solid, 99%. ^1H NMR (400 MHz, CDCl_3) δ 8.38 (s, 1H), 8.04 (d, $J = 8.8$ Hz, 1H), 7.82 (d, $J = 8.9$ Hz, 1H), 7.56 (d, $J = 7.5$ Hz, 4H), 7.37 (p, $J = 7.5, 6.8$ Hz, 6H). ^{13}C NMR (100 MHz, CDCl_3) δ 154.17, 153.69, 141.73, 139.91, 138.72, 138.61, 133.49, 131.47, 130.53, 129.93, 129.87, 129.18, 129.11, 128.38, 128.36, 123.87. (known compound¹³)



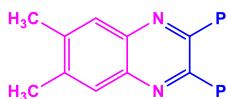
6-nitro-2,3-diphenylquinoxaline (Table S5, 5d): Light Yellow solid, 93%. ^1H NMR (400 MHz, CDCl_3) δ 9.03 (d, $J = 2.5$ Hz, 1H), 8.48 (dd, $J = 9.1, 2.5$ Hz, 1H), 8.26 (d, $J = 9.2$ Hz, 1H), 7.60 – 7.53 (m, 4H), 7.45 – 7.32 (m, 6H). ^{13}C NMR (100 MHz, CDCl_3) δ 156.28, 155.65, 147.78, 143.54, 139.91, 138.05, 137.99, 130.76, 129.93, 129.85, 129.82, 129.67, 128.49, 125.60, 123.29. (known compound¹⁴)



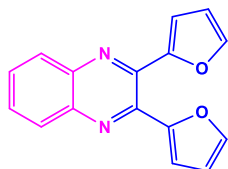
6-methyl-2,3-diphenylquinoxaline (Table S5, 5e): White solid, 99%. ^1H NMR (400 MHz, CDCl_3) δ 8.02 (d, $J = 8.5$ Hz, 1H), 7.91 (s, 1H), 7.49 (d, $J = 7.4$ Hz, 5H), 7.27 (d, $J = 6.9$ Hz, 6H), 2.51 (s, 3H). ^{13}C NMR (100 MHz, CDCl_3) δ 153.27, 152.53, 141.30, 140.45, 139.73, 139.27, 132.32, 129.95, 129.93, 128.74, 128.68, 128.28, 128.06, 22.02. (known compound¹⁴)



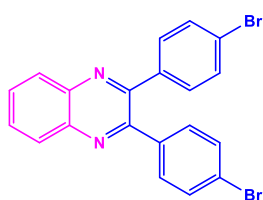
6-methoxy-2,3-diphenylquinoxaline (Table S5, 5f): Purple solid, 95%. ^1H NMR (400 MHz, CDCl_3) δ 8.05 (d, $J = 9.1$ Hz, 1H), 7.51 (dt, $J = 7.4, 3.7$ Hz, 4H), 7.46 (d, $J = 2.7$ Hz, 1H), 7.40 (dd, $J = 9.1, 2.8$ Hz, 1H), 7.37 – 7.26 (m, 6H), 3.95 (s, 3H). ^{13}C NMR (100 MHz, CDCl_3) δ 160.66, 153.10, 150.69, 142.52, 139.03, 138.98, 137.18, 129.95, 129.64, 128.51, 128.29, 128.08, 128.05, 123.20, 106.20, 55.67. (known compound¹⁴)



6,7-dimethyl-2,3-diphenylquinoxaline (Table S5, 5j): White solid, 99%. ^1H NMR (400 MHz, CDCl_3) δ 7.95 (s, 2H), 7.54 (dd, $J = 7.4, 2.2$ Hz, 4H), 7.38 – 7.31 (m, 6H), 2.52 (s, 6H). ^{13}C NMR (100 MHz, CDCl_3) δ 152.47, 140.55, 140.21, 139.38, 129.89, 128.57, 128.23, 128.21, 20.53, 20.51. (known compound¹³)



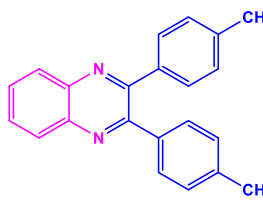
2,3-di(furan-2-yl)quinoxaline (Table S5, 5h): Pale brown solid, 94%. Pale brown solid, 94%. ^1H NMR (400 MHz, CDCl_3) δ 8.13 (dt, $J = 7.0, 3.5$ Hz, 2H), 7.75 (dd, $J = 6.4, 3.4$ Hz, 2H), 7.63 (d, $J = 1.7$ Hz, 2H), 6.66 (d, $J = 3.4$ Hz, 2H), 6.57 (dd, $J = 3.5, 1.8$ Hz, 2H). ^{13}C NMR (100 MHz, CDCl_3) δ 150.72, 144.26, 142.62, 140.59, 130.44, 129.10, 113.06, 111.96. (known compound¹⁵)



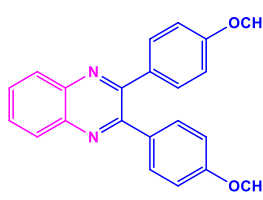
2,3-bis(4-bromophenyl)quinoxaline (Table S5, 5i): White solid, 96%. ^1H NMR (400 MHz, CDCl_3) δ 8.13 (dt, $J = 7.0, 3.5$ Hz, 2H), 7.77 (dt, $J = 6.4, 3.6$ Hz, 2H), 7.48 (d, $J = 8.2$ Hz, 4H), 7.38 (d, $J = 8.3$ Hz, 4H). ^{13}C NMR (100 MHz, CDCl_3) δ 151.88, 141.21, 137.63, 131.70, 131.56, 131.47, 130.44, 129.20, 123.74. (known compound¹²)



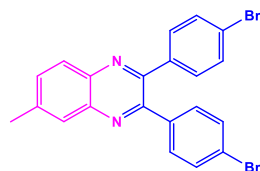
2,3-bis(4-fluorophenyl)quinoxaline (Table S5, 5j): Light yellow solid, 96%. ^1H NMR (400 MHz, CDCl_3) δ 8.11 (dd, $J = 6.4, 3.5$ Hz, 2H), 7.72 (dt, $J = 6.4, 3.5$ Hz, 2H), 7.48 (dd, $J = 8.6, 5.4$ Hz, 4H), 7.02 (t, $J = 8.6$ Hz, 4H). ^{13}C NMR (100 MHz, CDCl_3) δ 164.42, 161.94, 152.09, 141.13, 134.98, 134.95, 131.86, 131.78, 130.18, 129.11, 115.62, 115.40. (known compound¹⁶)



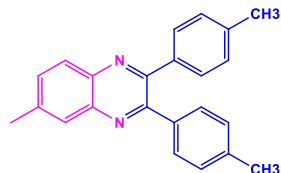
2,3-di-p-tolylquinoxaline (Table S5, 5k): White solid, 99%. ^1H NMR (400 MHz, CDCl_3) δ 8.13 (dt, $J = 6.8, 3.4$ Hz, 2H), 7.70 (dt, $J = 6.4, 3.4$ Hz, 2H), 7.43 (d, $J = 8.0$ Hz, 4H), 7.13 (d, $J = 7.9$ Hz, 4H), 2.34 (s, 6H). ^{13}C NMR (101 MHz, CDCl_3) δ 153.50, 141.17, 138.77, 136.41, 129.79, 129.71, 129.15, 129.03, 21.44, 21.42. (known compound¹²)



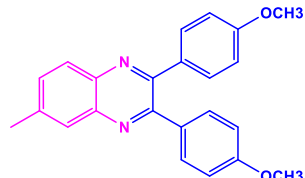
2,3-bis(4-methoxyphenyl)quinoxaline (Table S5, 5l): White solid, 90%. ^1H NMR (400 MHz, CDCl_3) δ 7.97 (dt, $J = 7.0, 3.5$ Hz, 2H), 7.55 (dp, $J = 6.9, 3.8$ Hz, 2H), 7.39 – 7.33 (m, 4H), 6.75 – 6.70 (m, 4H), 3.64 (s, 6H). ^{13}C NMR (100 MHz, CDCl_3) δ 160.14, 152.98, 141.04, 131.68, 131.30, 129.55, 128.99, 113.76, 55.30, 55.28. (known compound¹²)



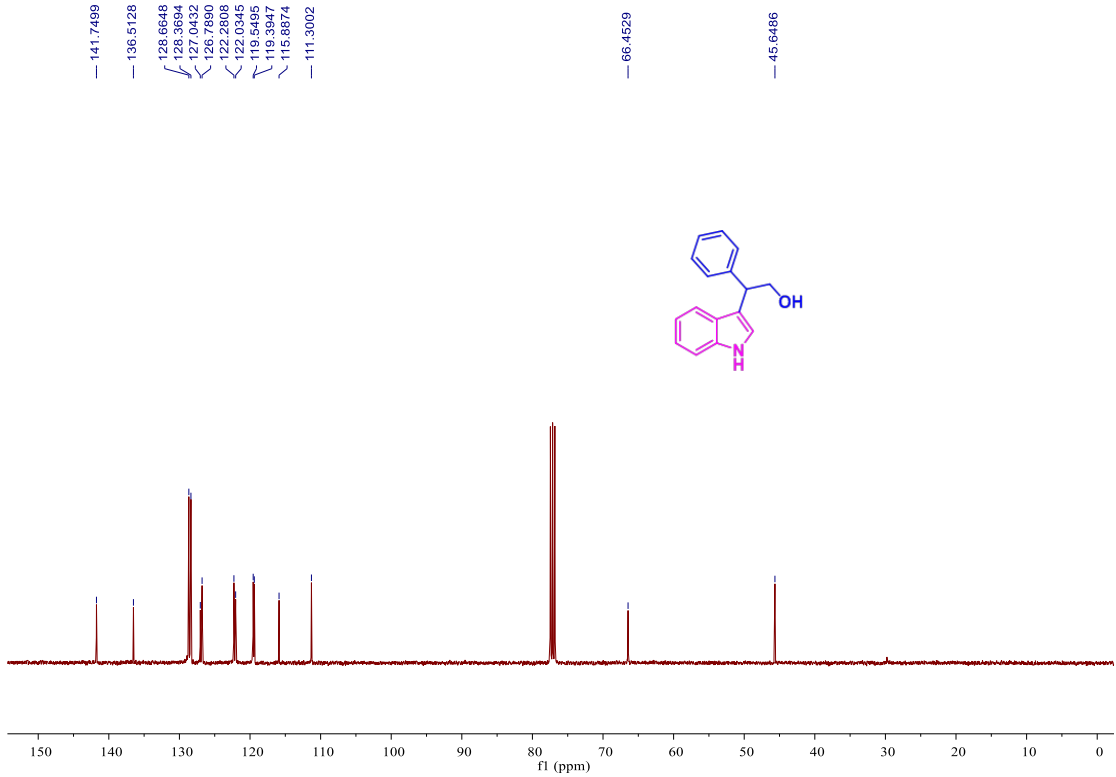
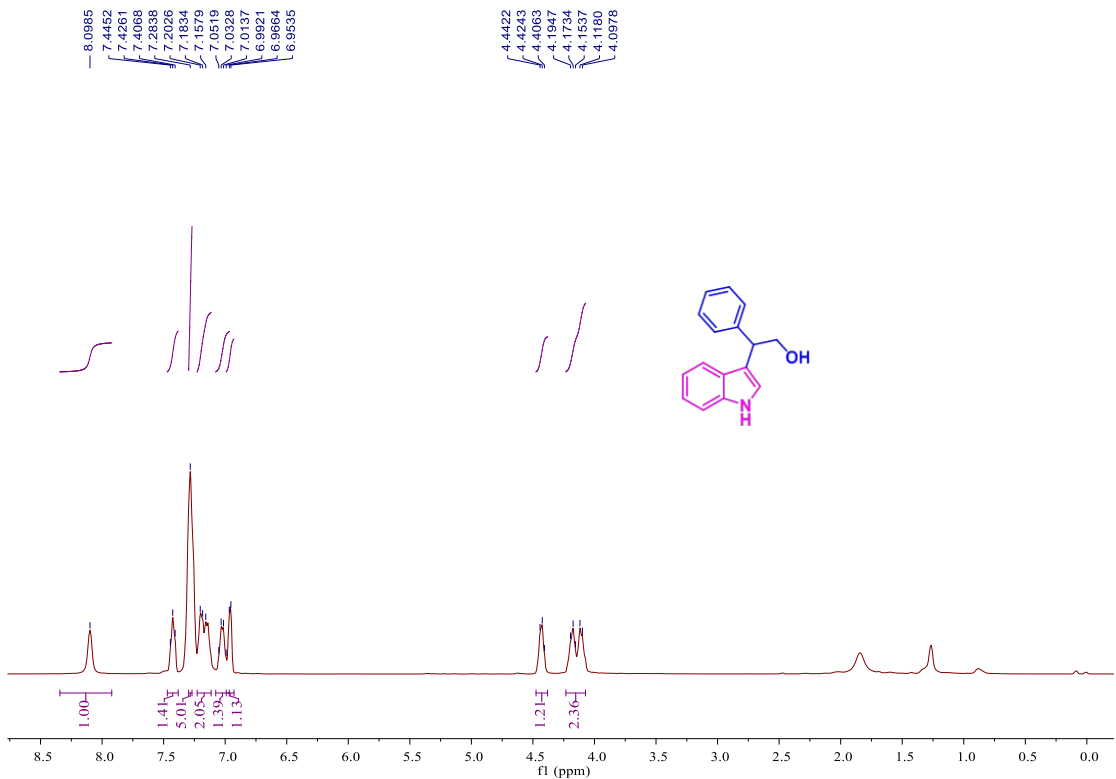
2,3-bis(4-bromophenyl)-6-methylquinoxaline (Table S5, 5l): White solid, 96%. ^1H NMR (400 MHz, CDCl_3) δ 8.00 (d, $J = 8.5$ Hz, 1H), 7.89 (d, $J = 1.5$ Hz, 1H), 7.58 (dd, $J = 8.6, 2.0$ Hz, 1H), 7.49 – 7.43 (m, 4H), 7.38 – 7.33 (m, 4H), 2.58 (s, 3H). ^{13}C NMR (100 MHz, CDCl_3) δ 151.69, 150.93, 141.27, 141.04, 139.71, 137.78, 132.79, 131.63, 131.47, 131.44, 128.68, 127.98, 123.59, 123.51, 22.04, 22.02. (known compound¹²)

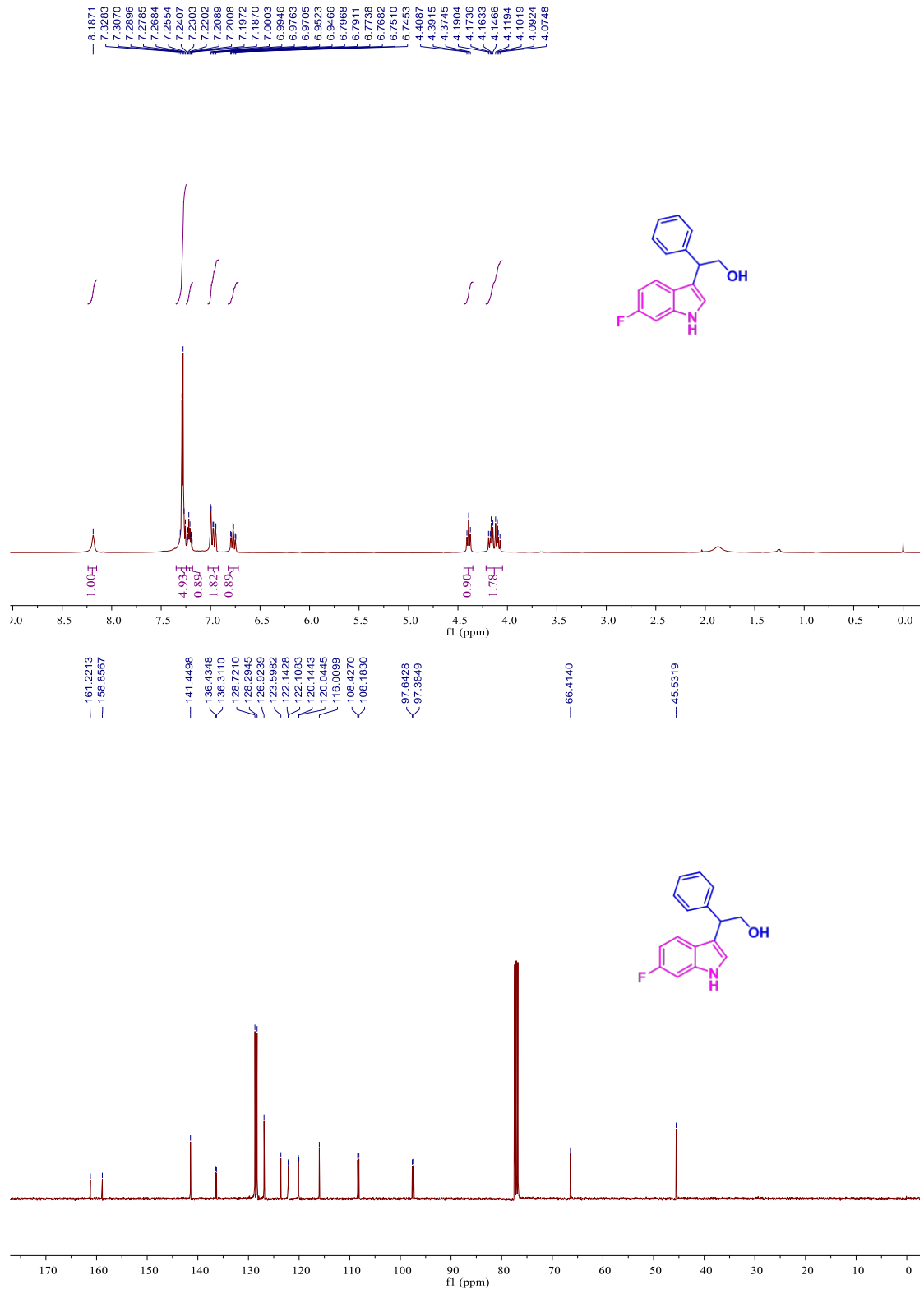


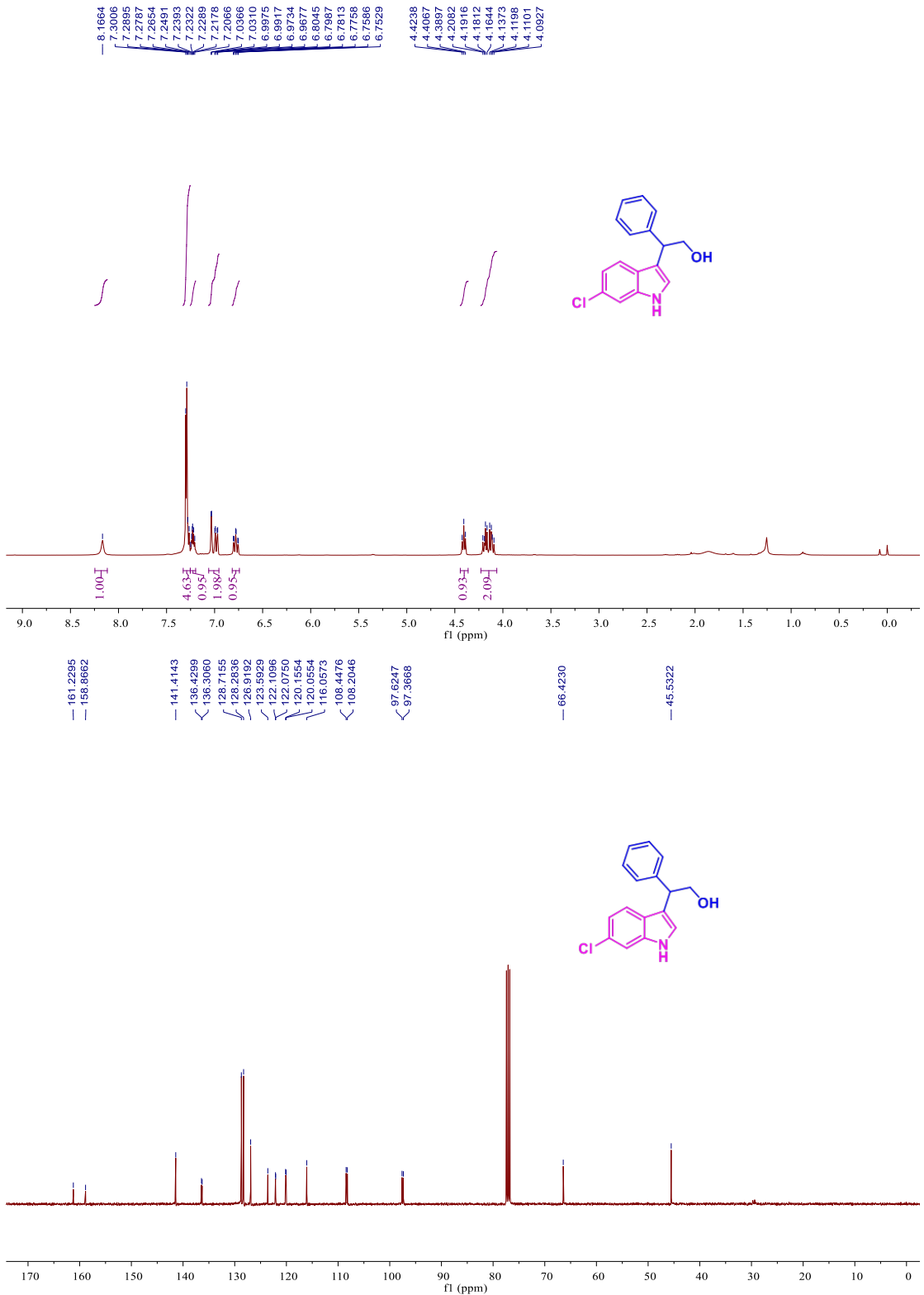
6-methyl-2,3-di-p-tolylquinoxaline (Table S5, 5l): White solid, 97%. ^1H NMR (400 MHz, CDCl_3) δ 8.00 (d, $J = 8.5$ Hz, 1H), 7.89 (s, 1H), 7.48 (dd, $J = 8.6, 1.9$ Hz, 1H), 7.41 (dd, $J = 8.2, 2.3$ Hz, 4H), 7.09 (d, $J = 7.9$ Hz, 4H), 2.52 (s, 3H), 2.31 (s, 6H). ^{13}C NMR (100 MHz, CDCl_3) δ 153.31, 152.58, 141.24, 140.09, 139.66, 138.58, 138.50, 136.60, 132.00, 129.84, 129.81, 128.98, 128.68, 128.01, 21.95, 21.93, 21.43, 21.40. (known compound¹²)

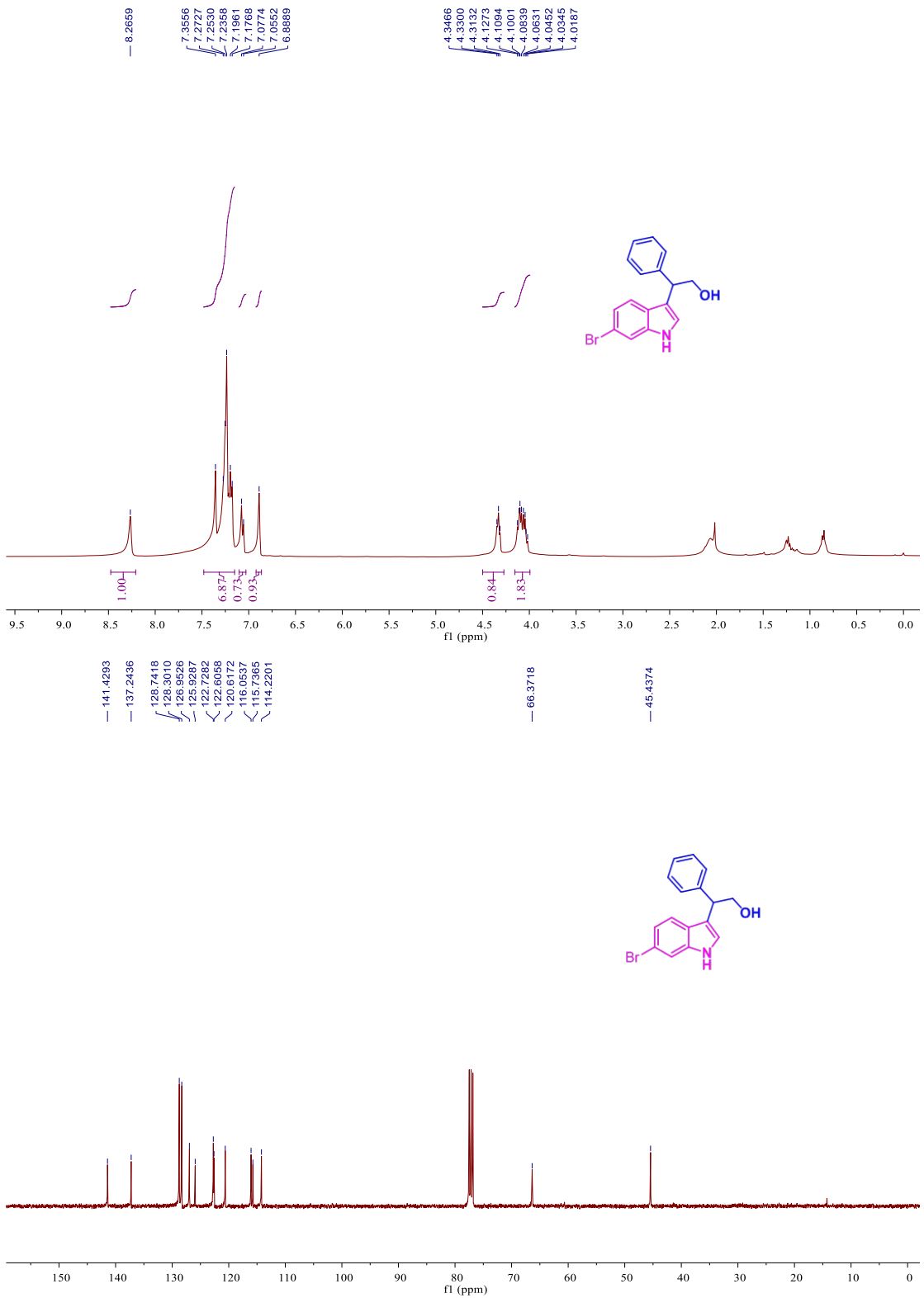


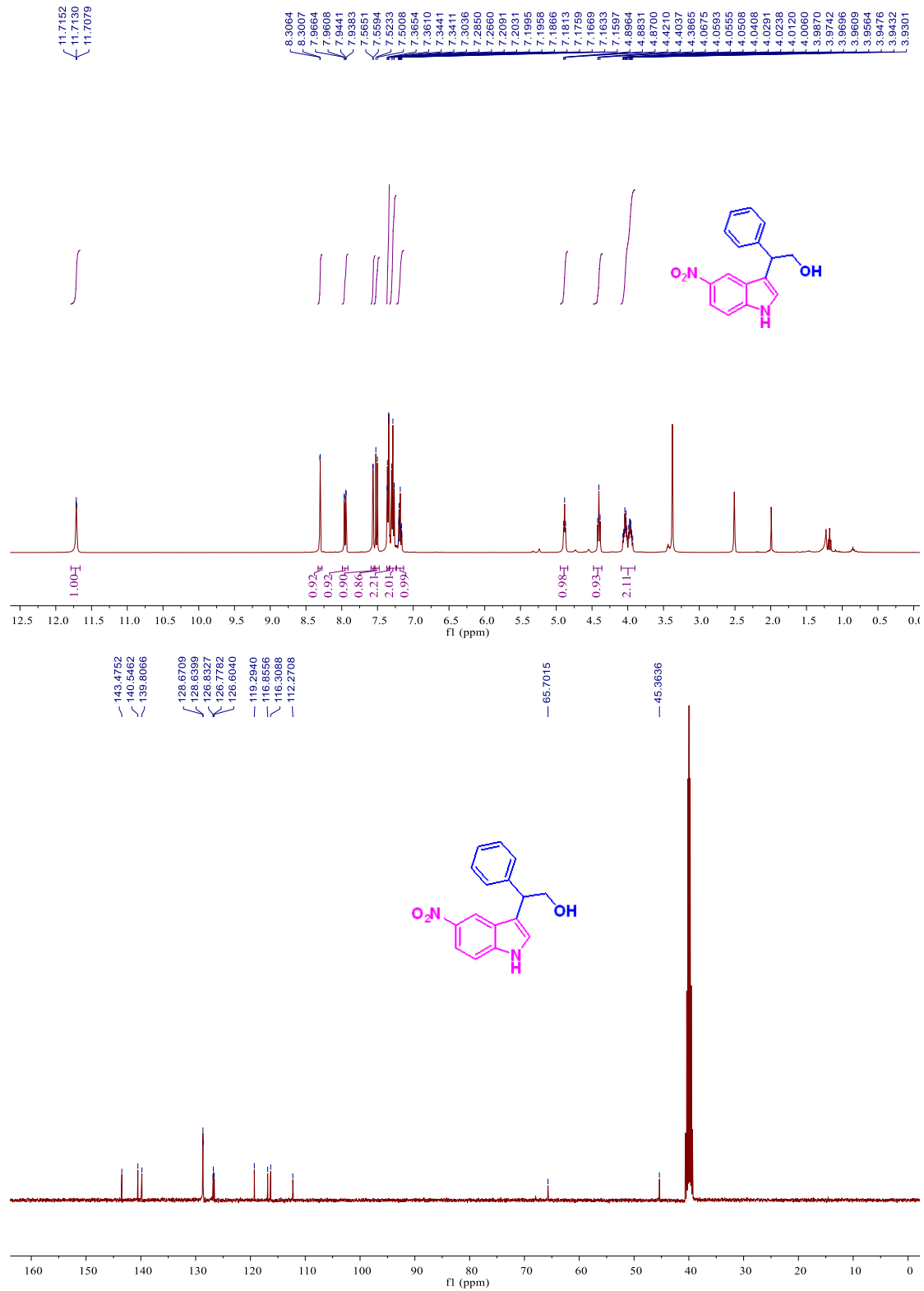
2,3-bis(4-methoxyphenyl)-6-methylquinoxaline (Table S5, 5l): White solid, 95%. ^1H NMR (400 MHz, CDCl_3) δ 7.97 (d, $J = 8.5$ Hz, 1H), 7.86 (s, 1H), 7.47 (ddd, $J = 8.8, 6.1, 2.3$ Hz, 5H), 6.83 (d, $J = 8.5$ Hz, 4H), 3.75 (s, 6H), 2.53 (s, 3H). ^{13}C NMR (100 MHz, CDCl_3) δ 160.06, 160.00, 152.80, 152.08, 141.09, 139.92, 139.50, 131.85, 131.83, 131.29, 131.25, 128.52, 127.86, 113.70, 55.27, 55.24, 21.90, 21.88. (known compound¹²)

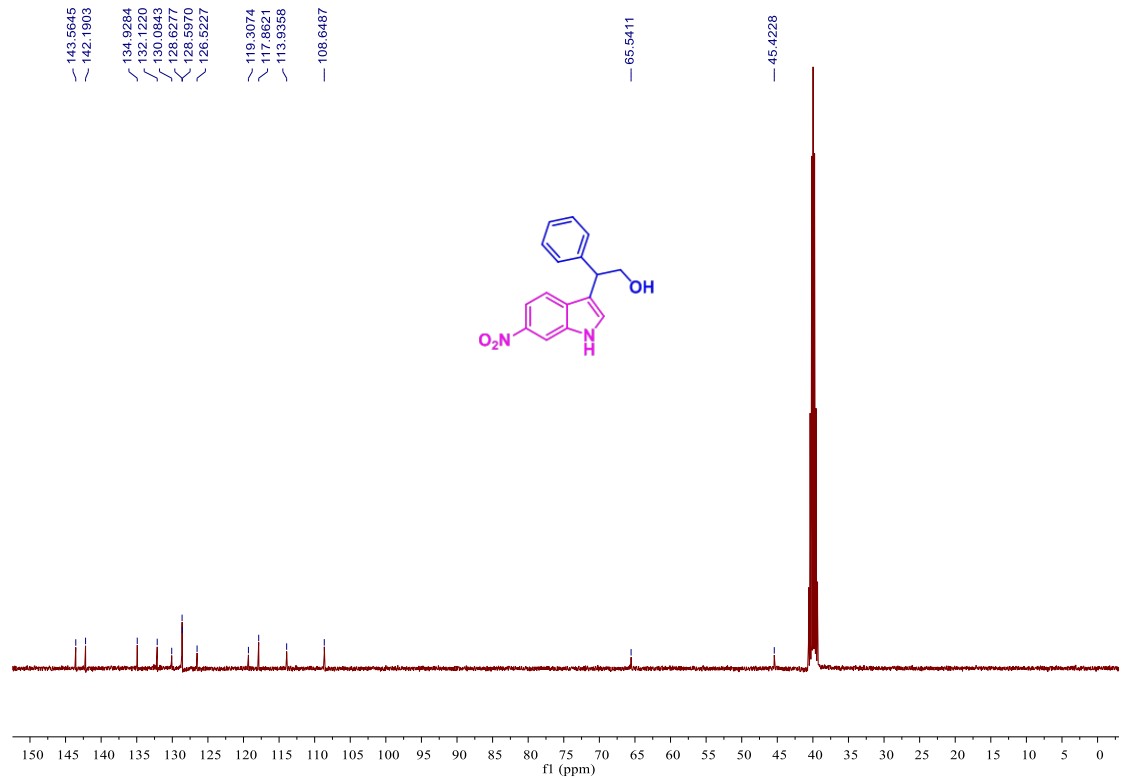
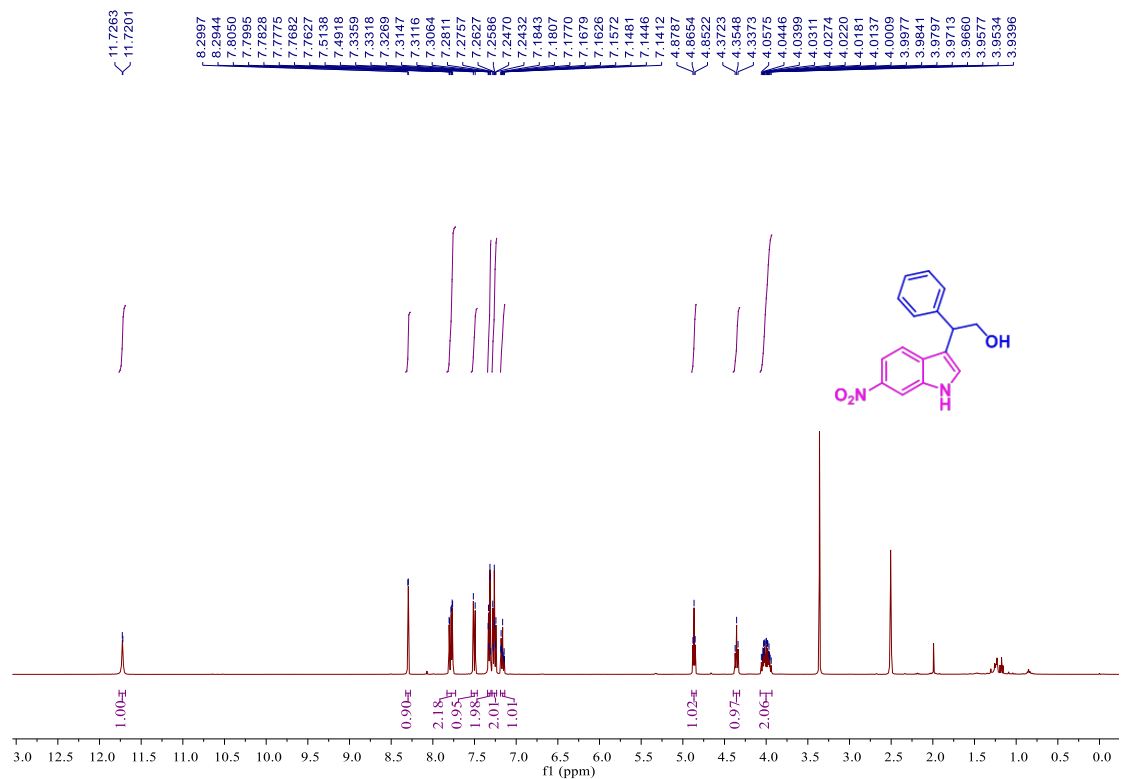


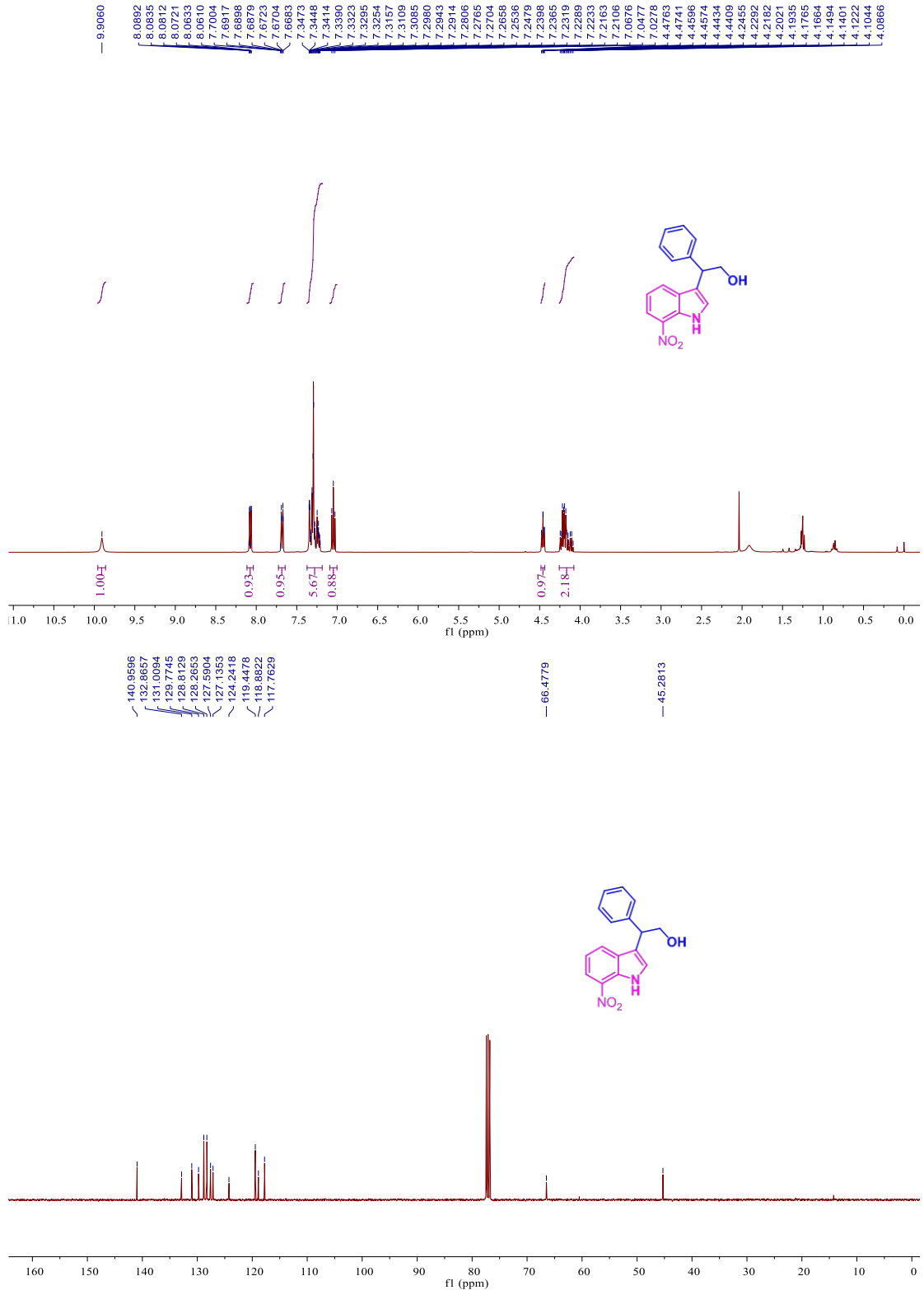


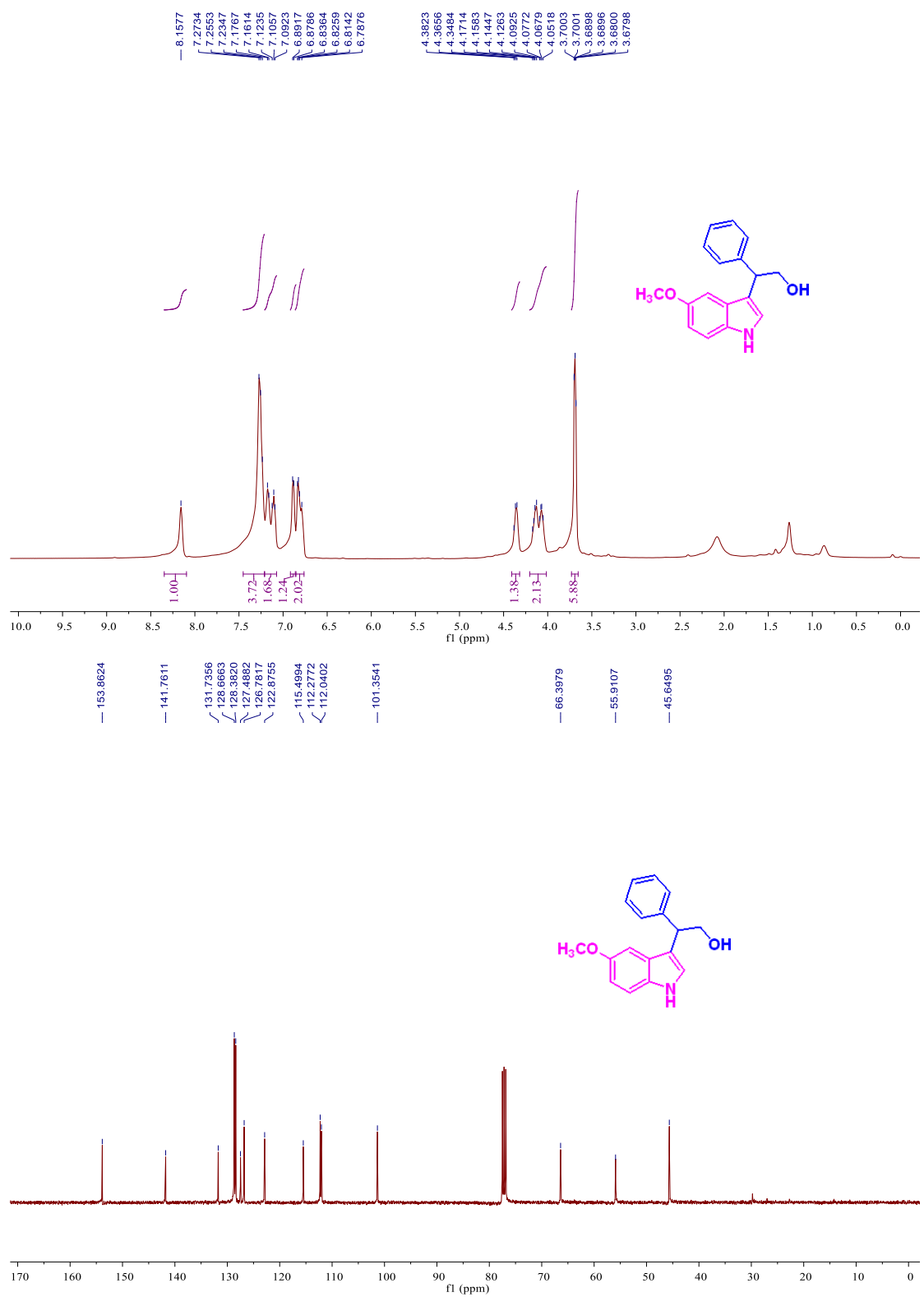


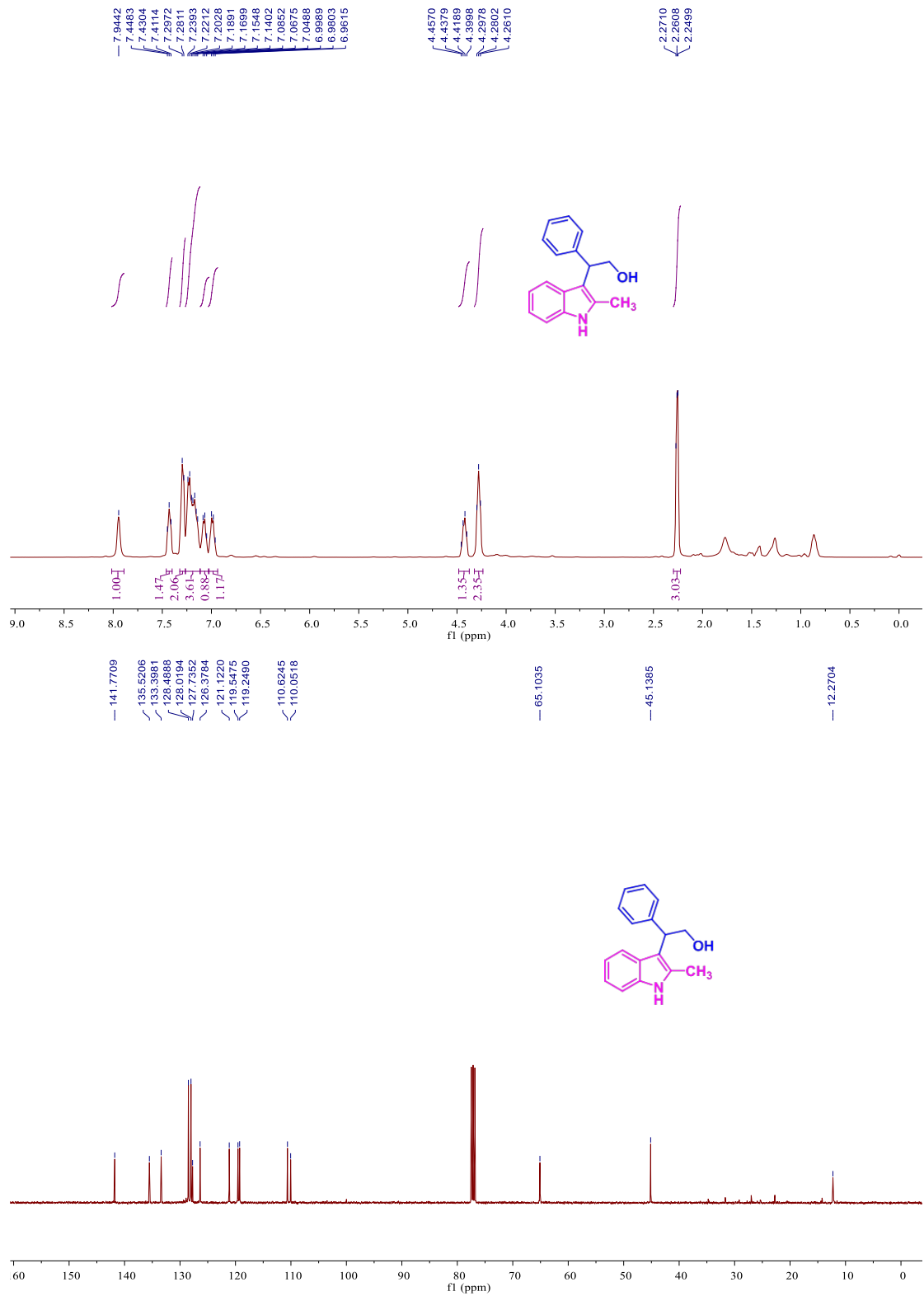


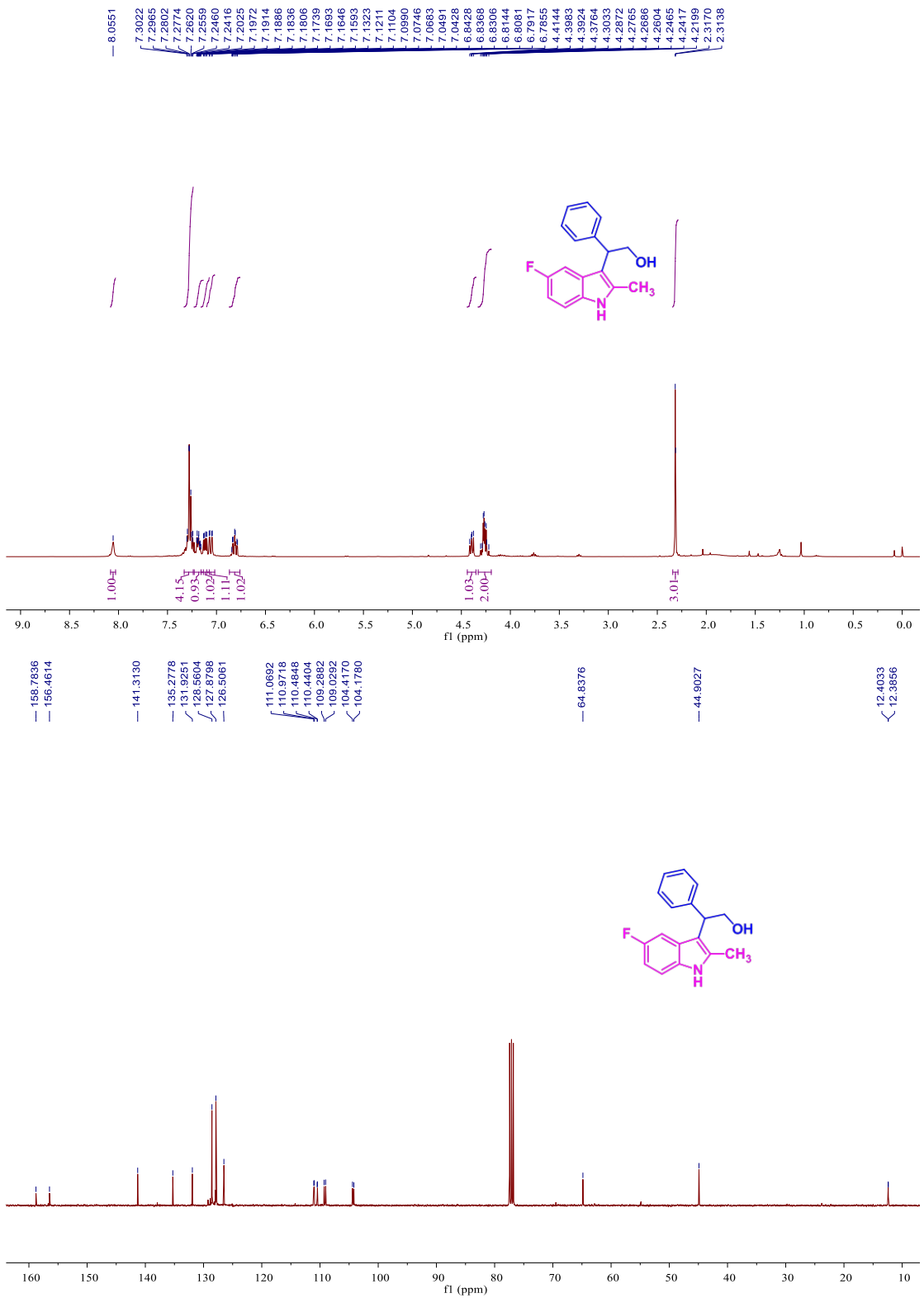


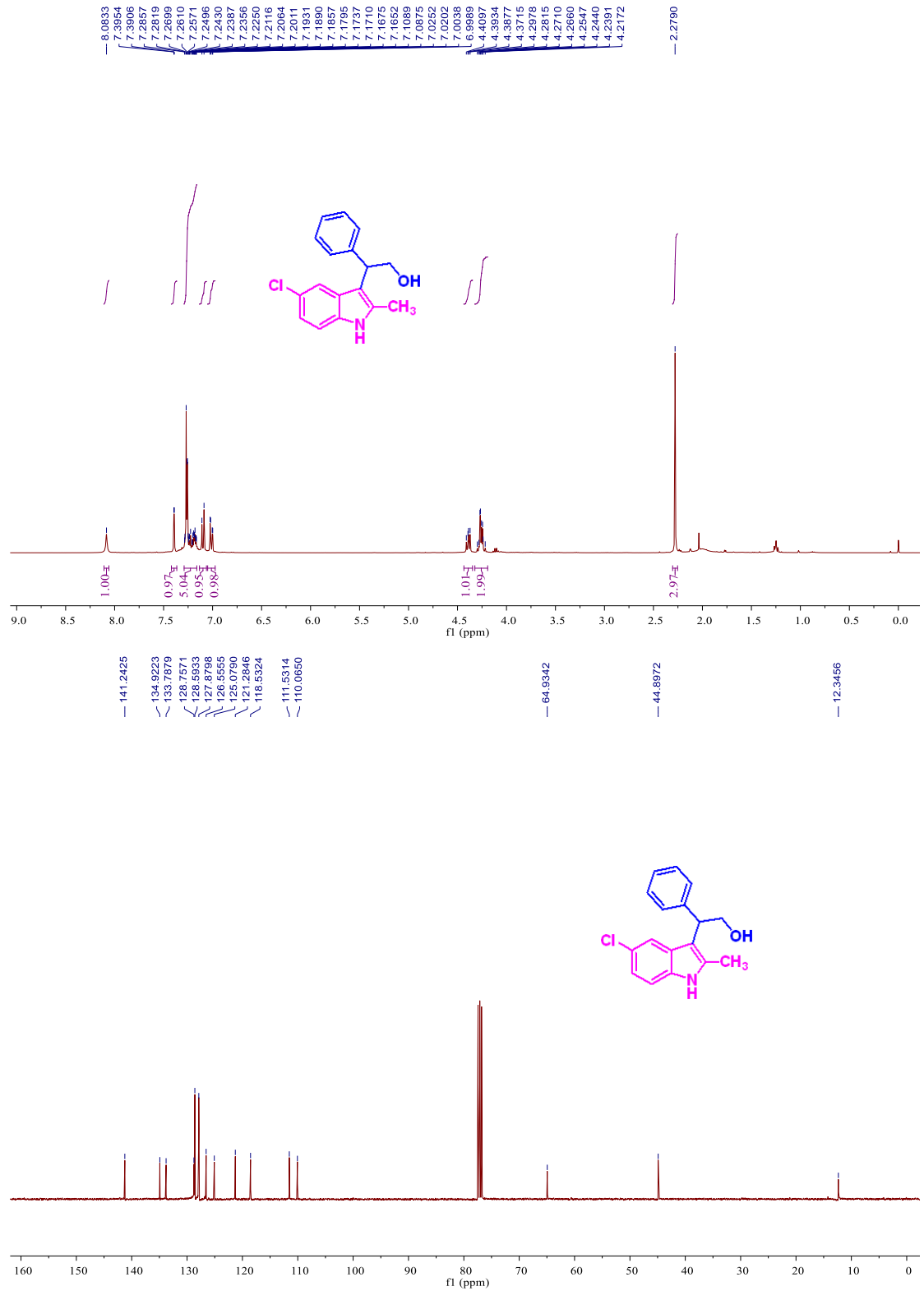


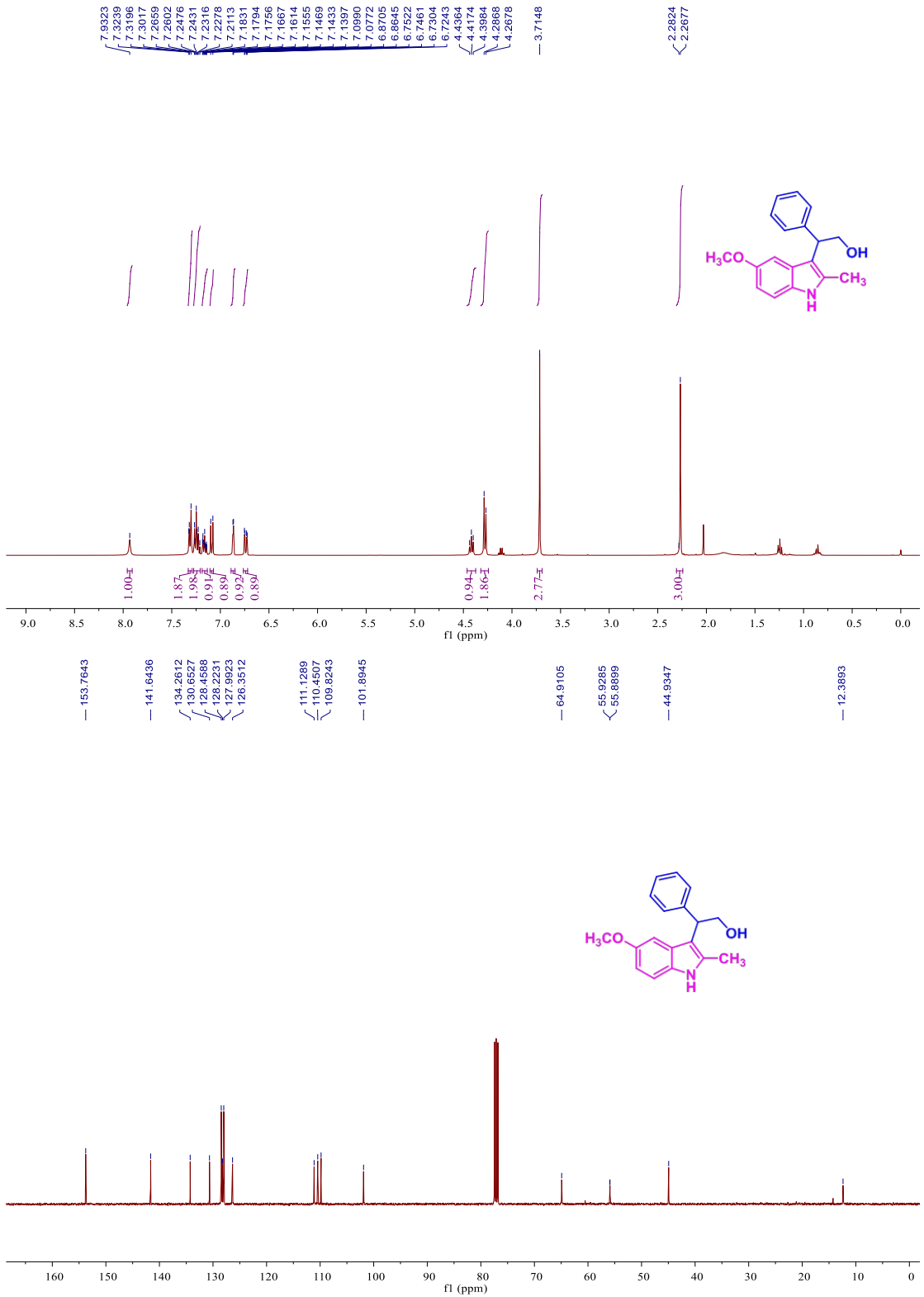


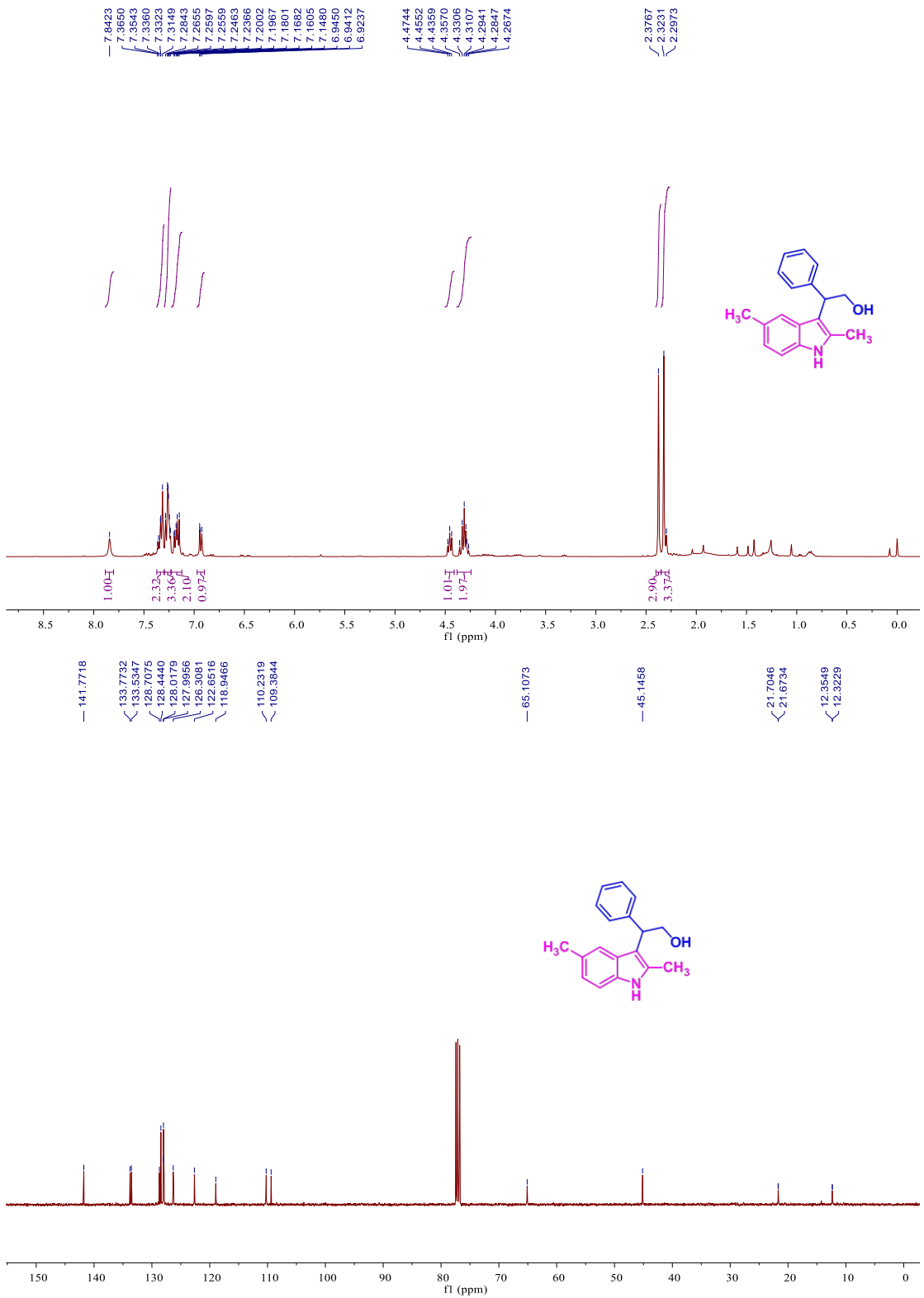


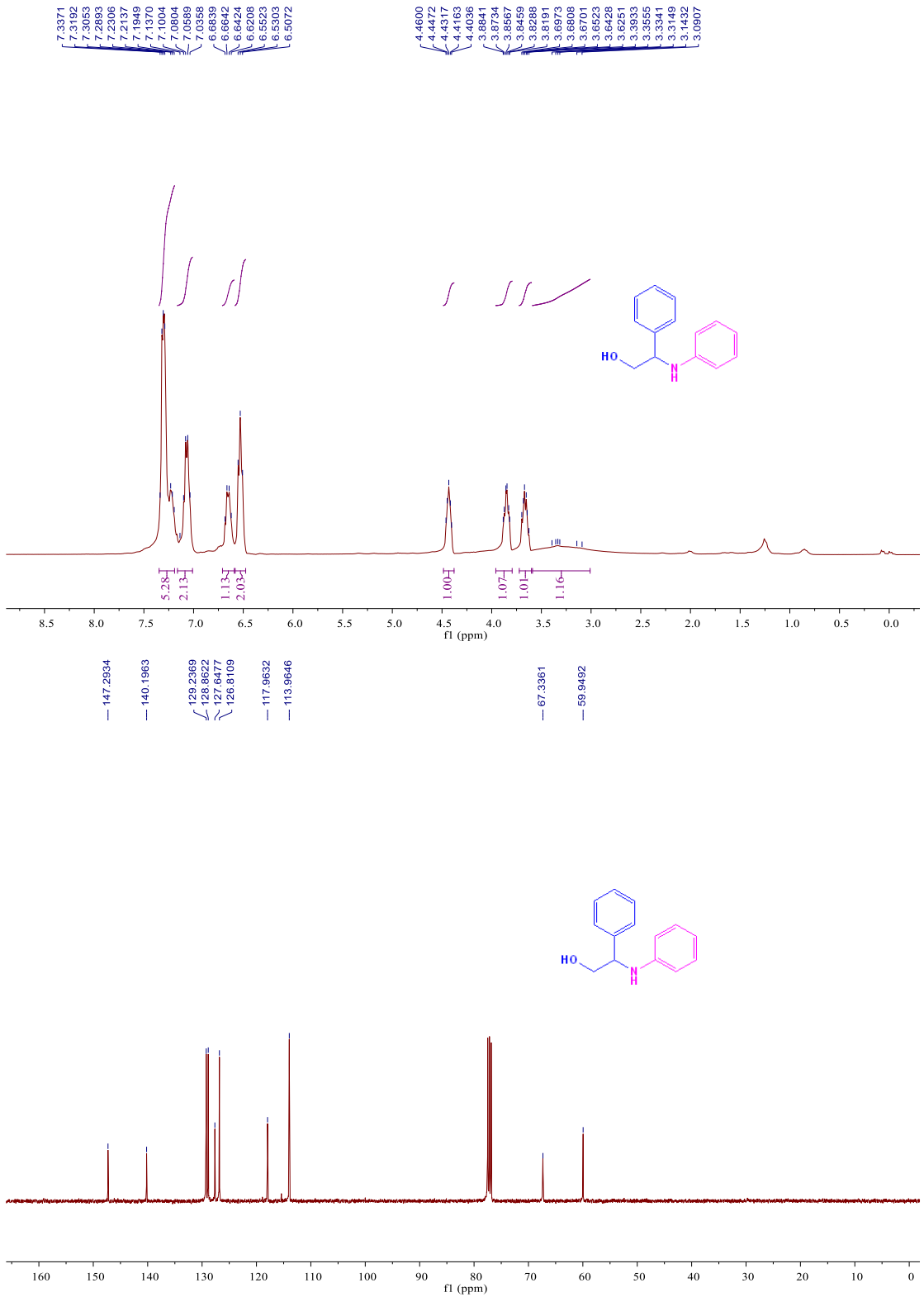


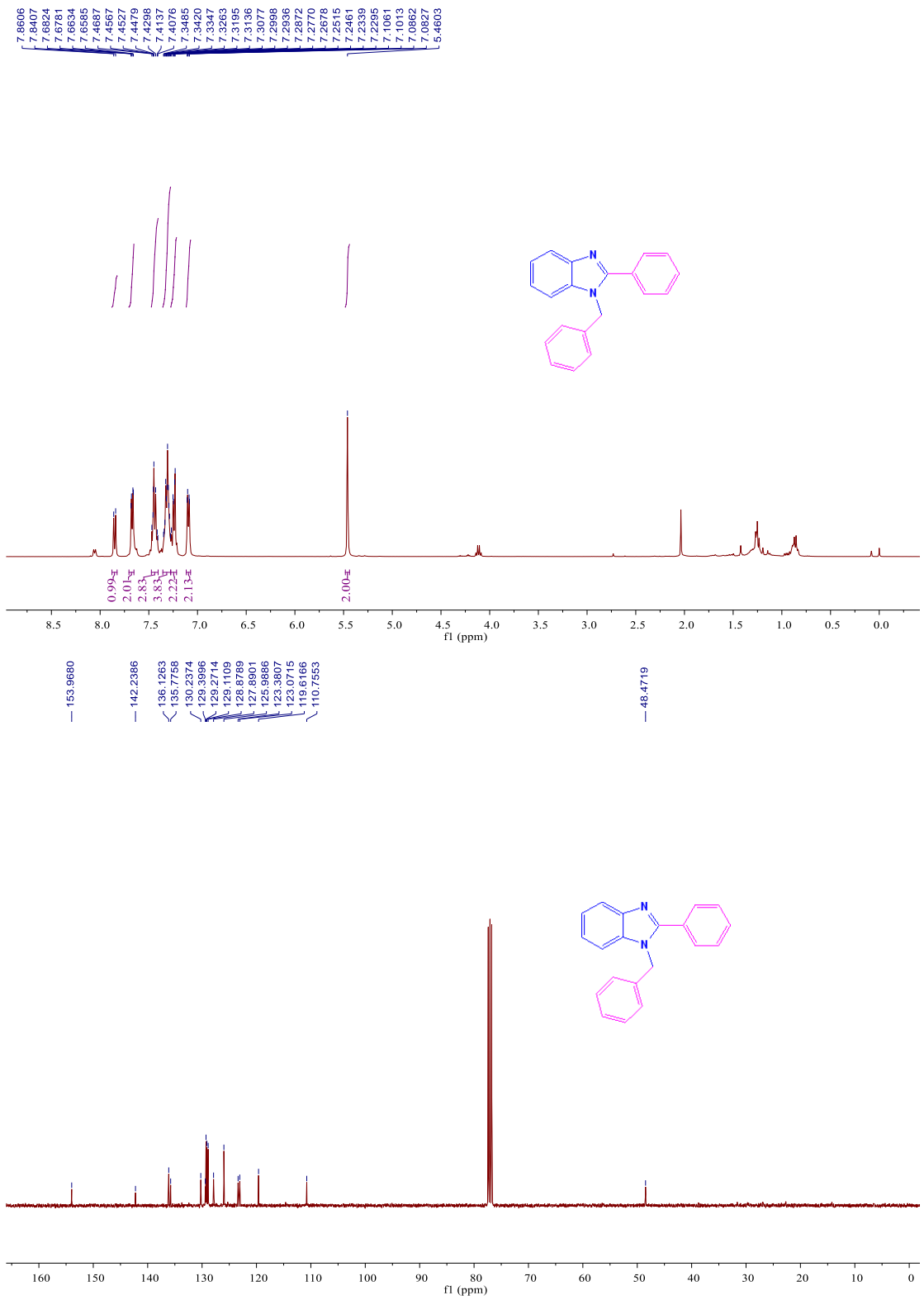


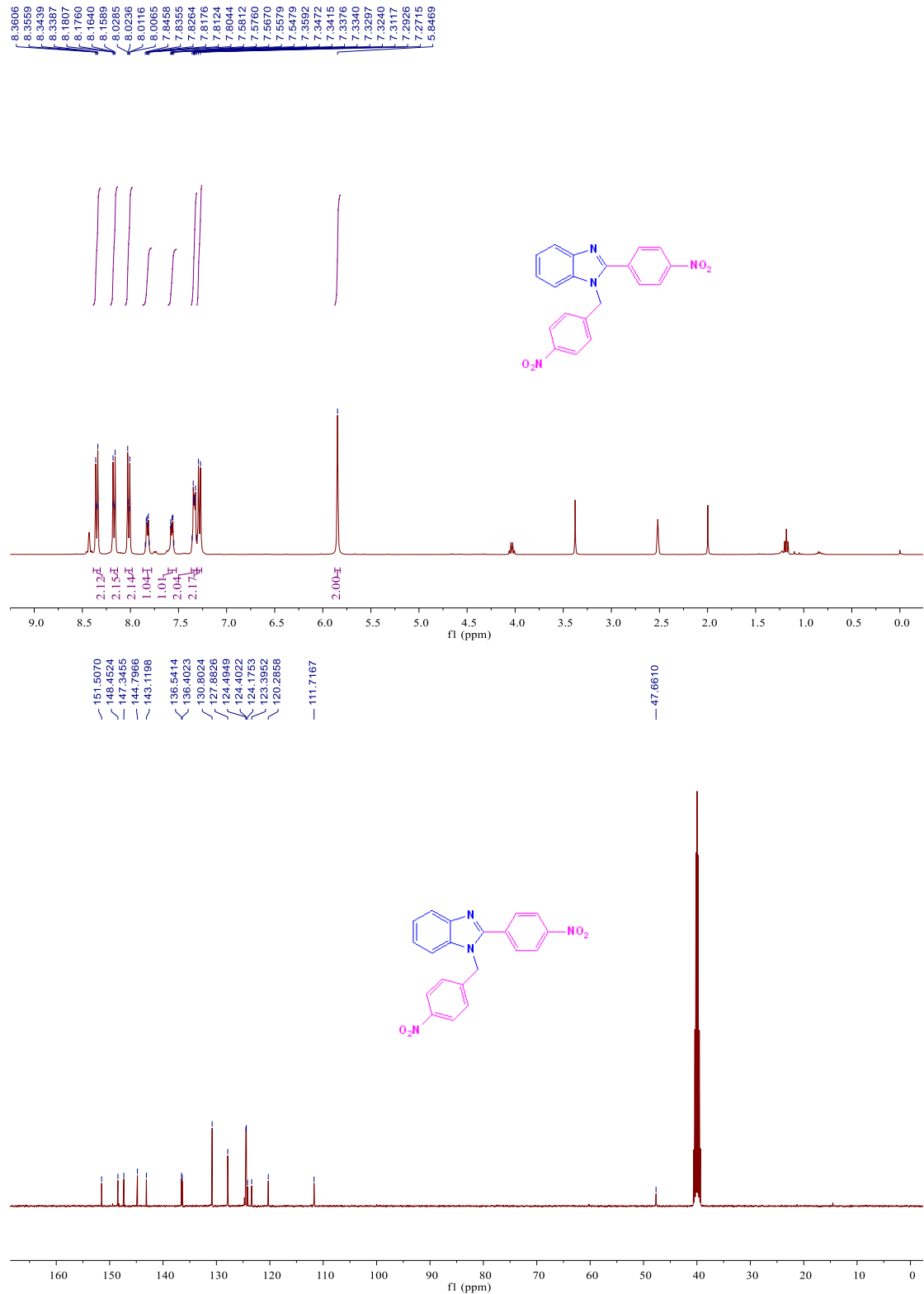


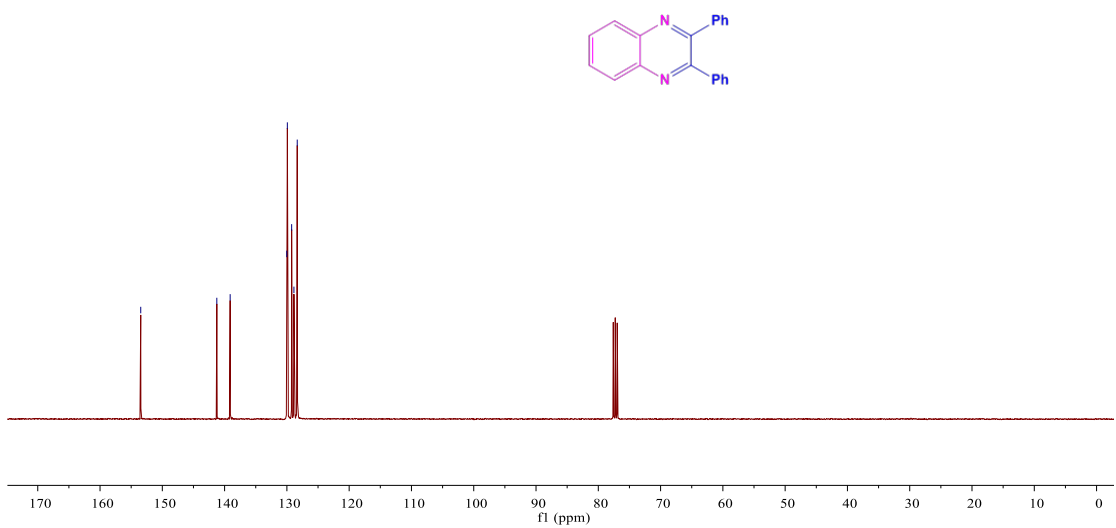
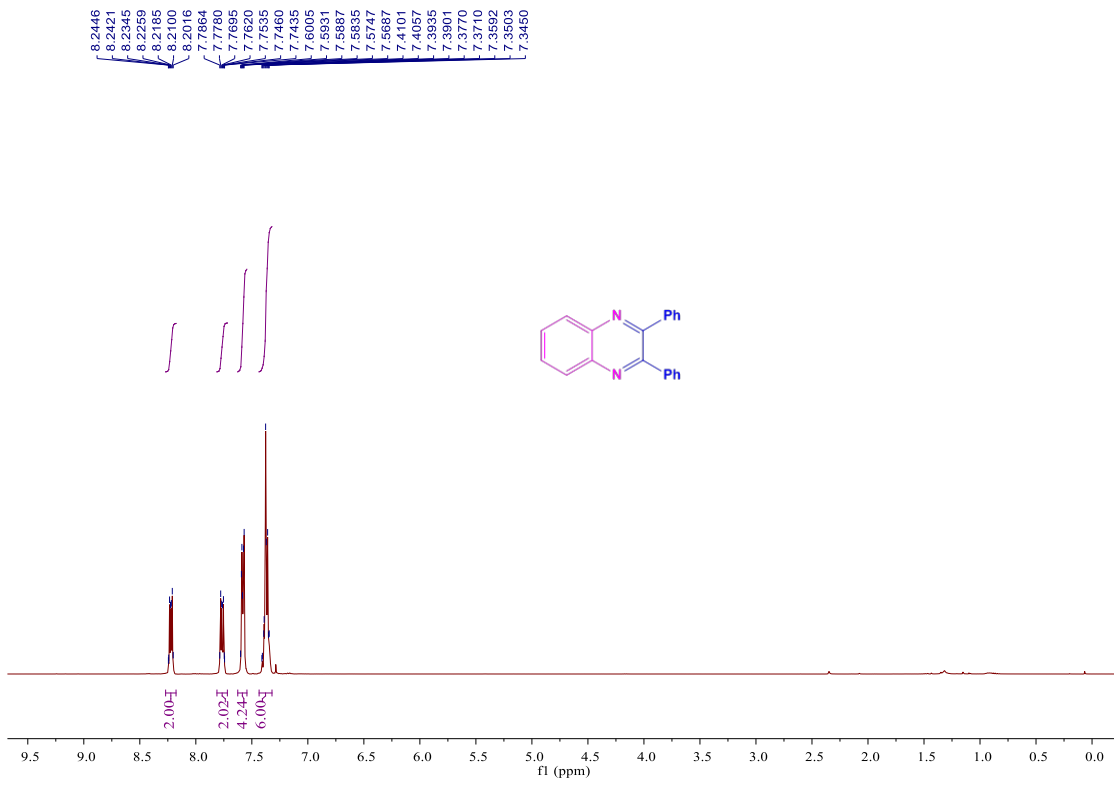


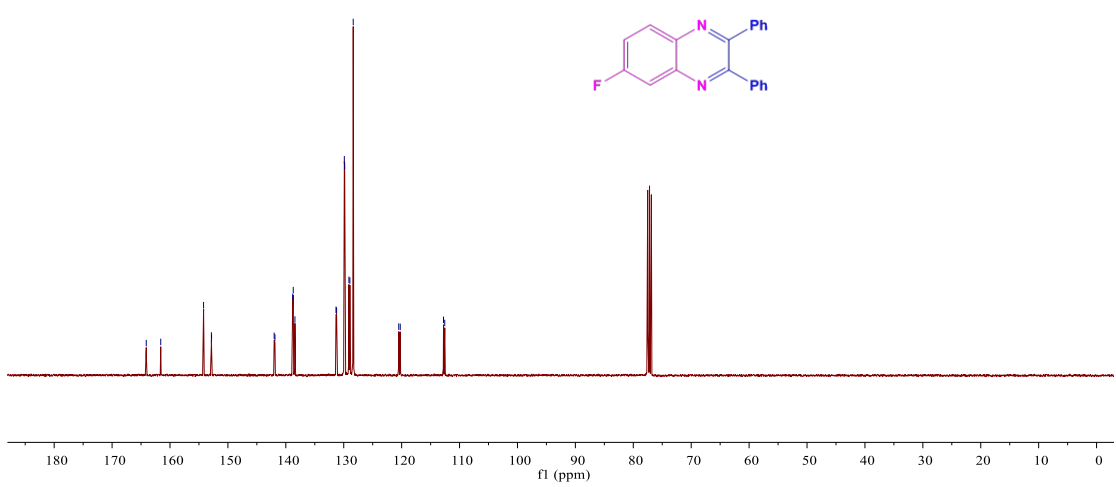
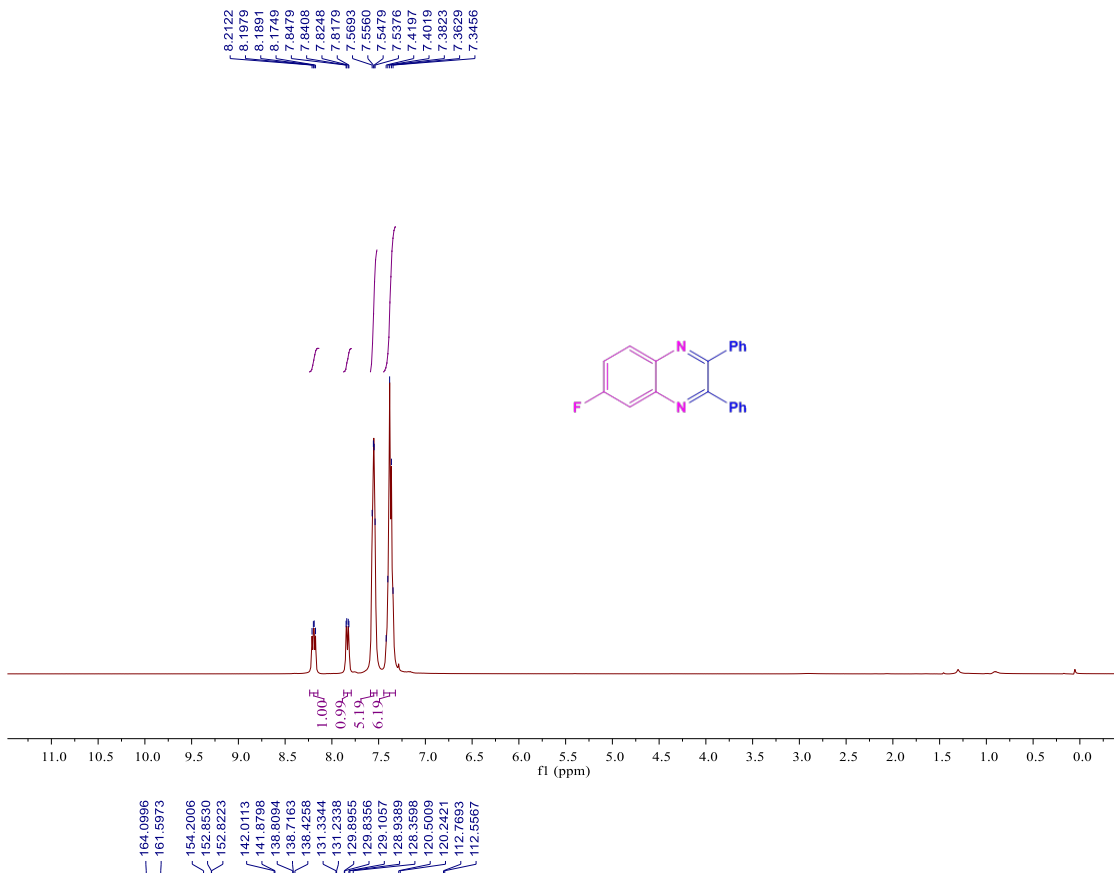


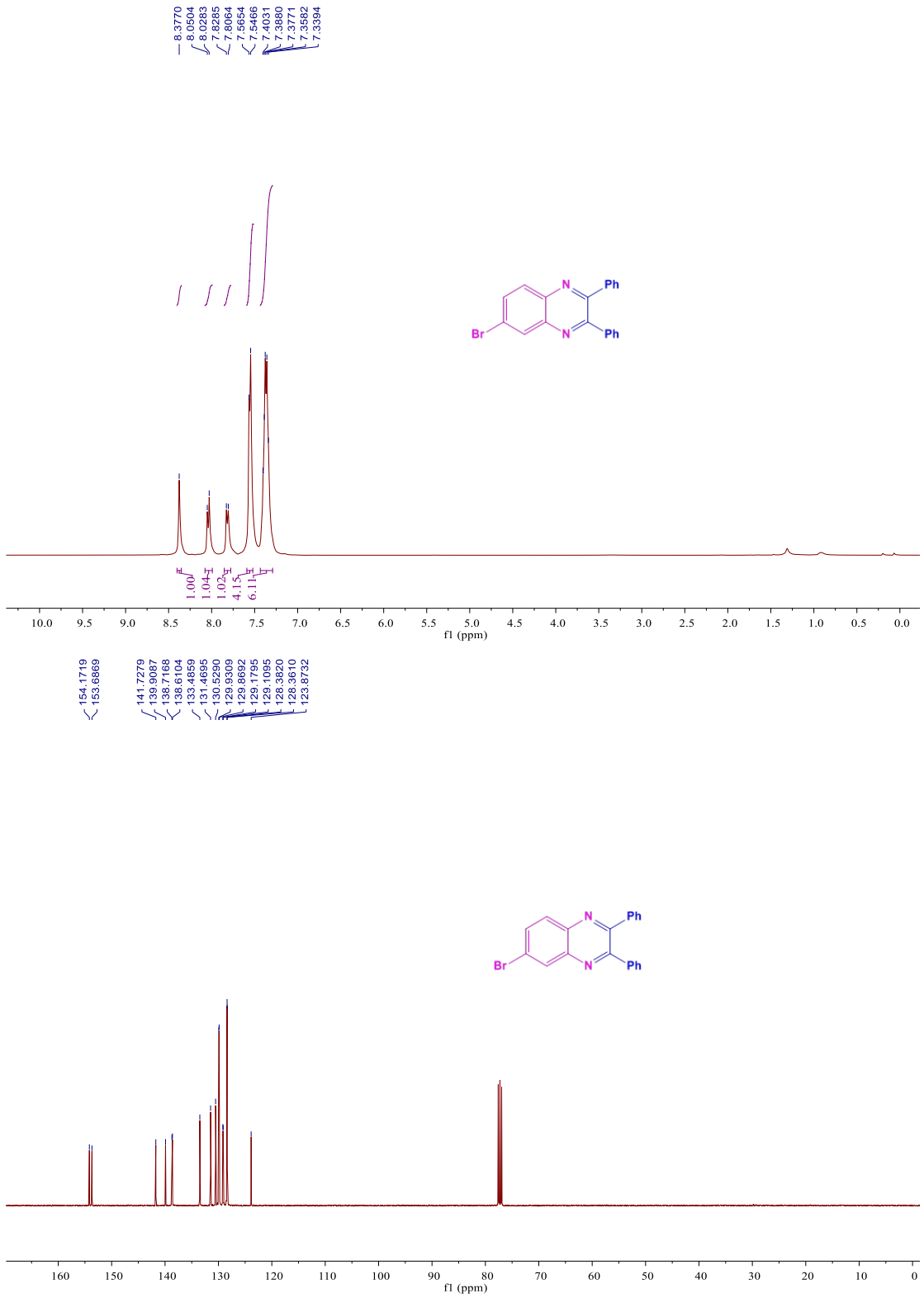


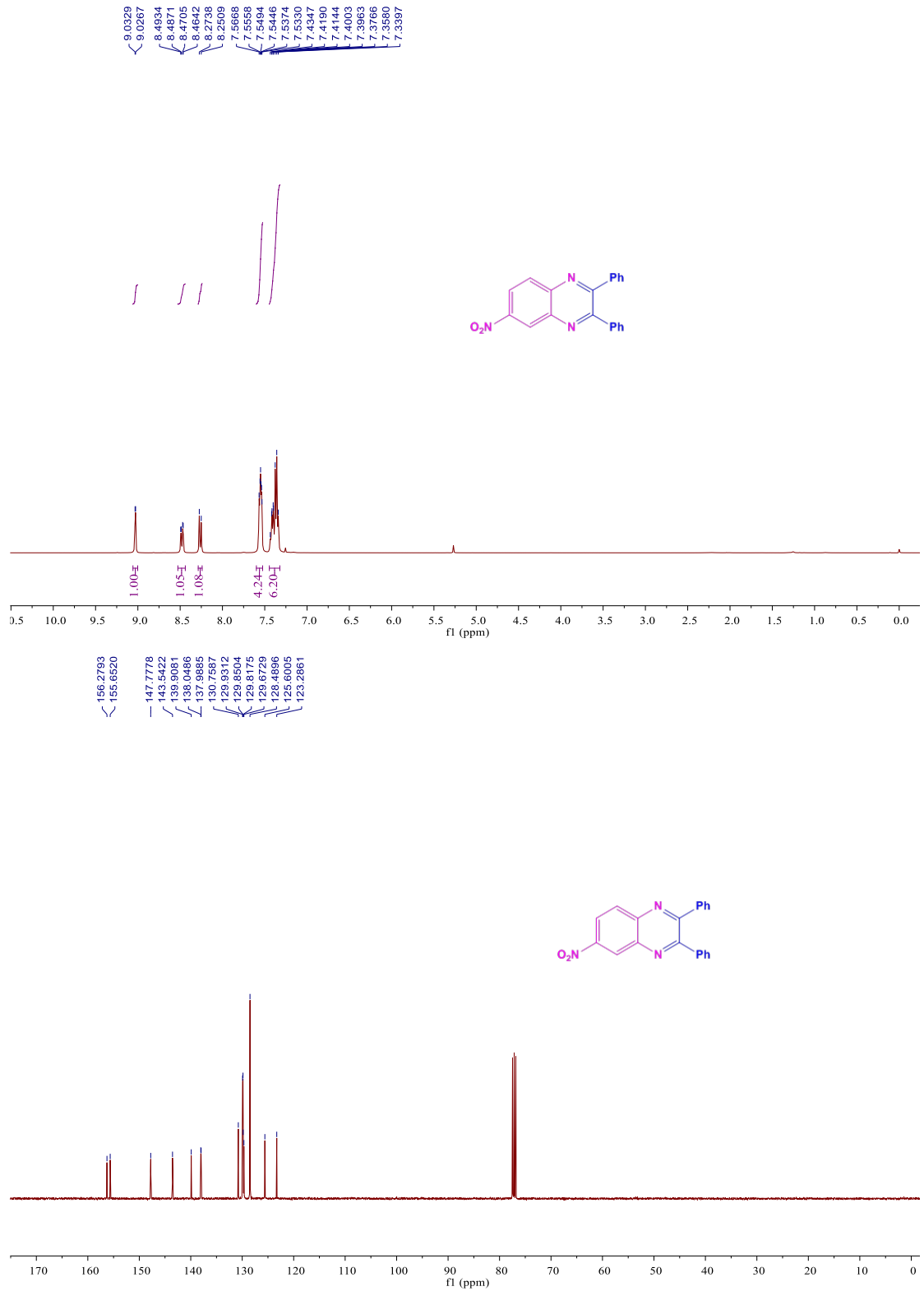


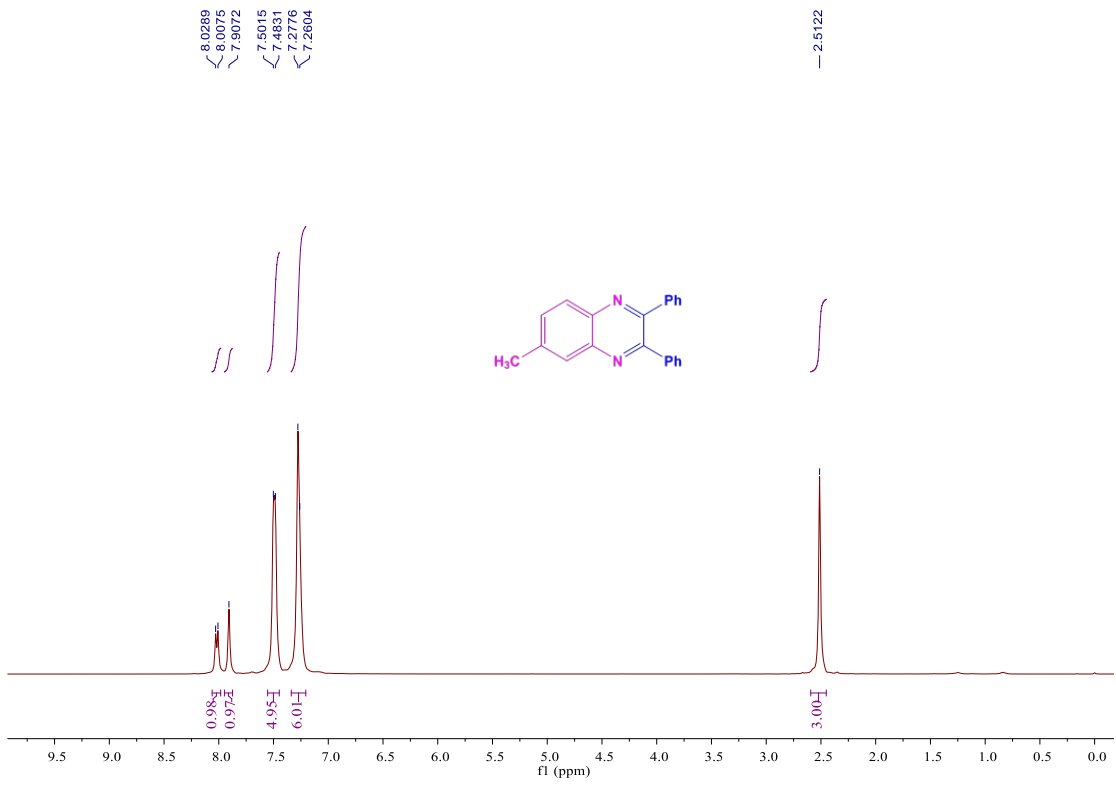




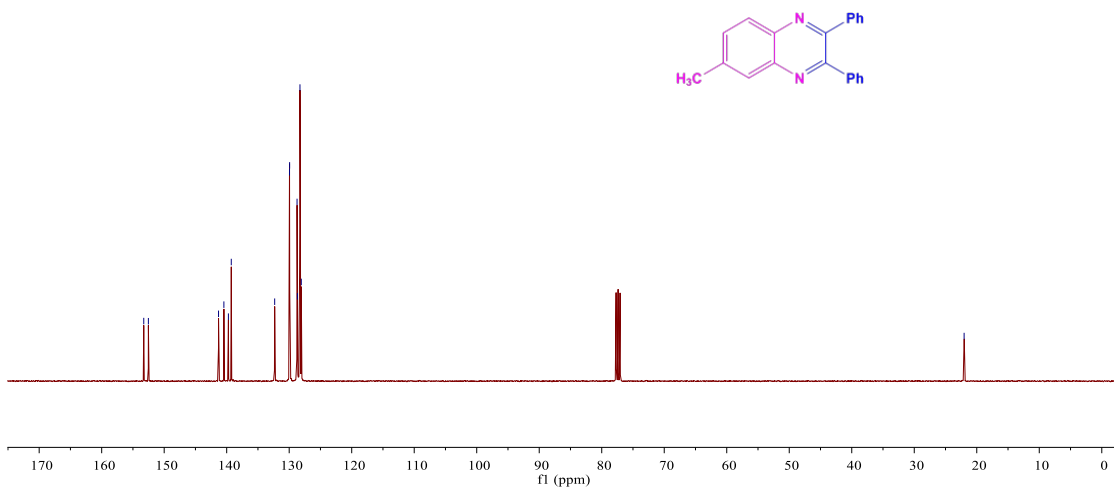


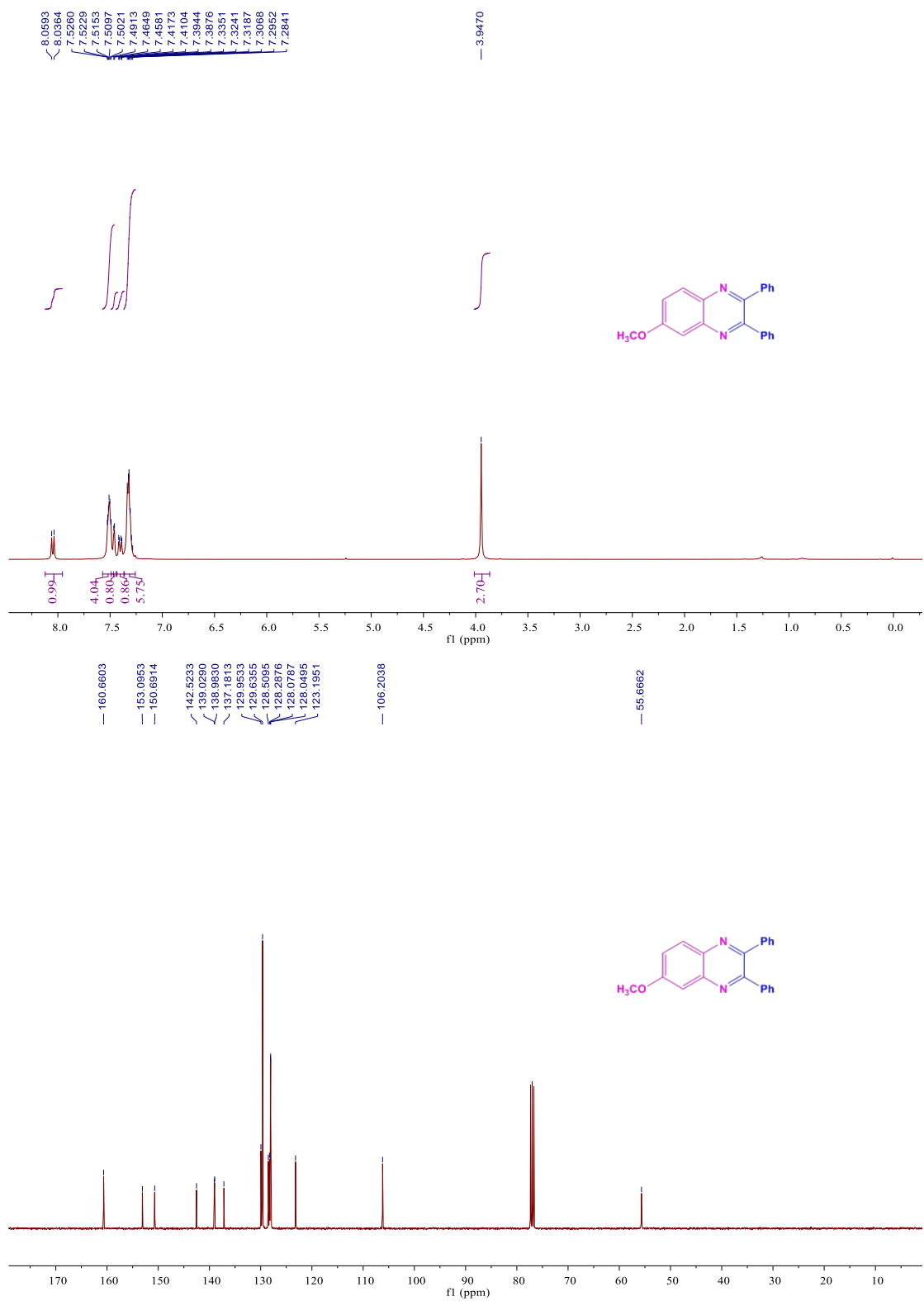


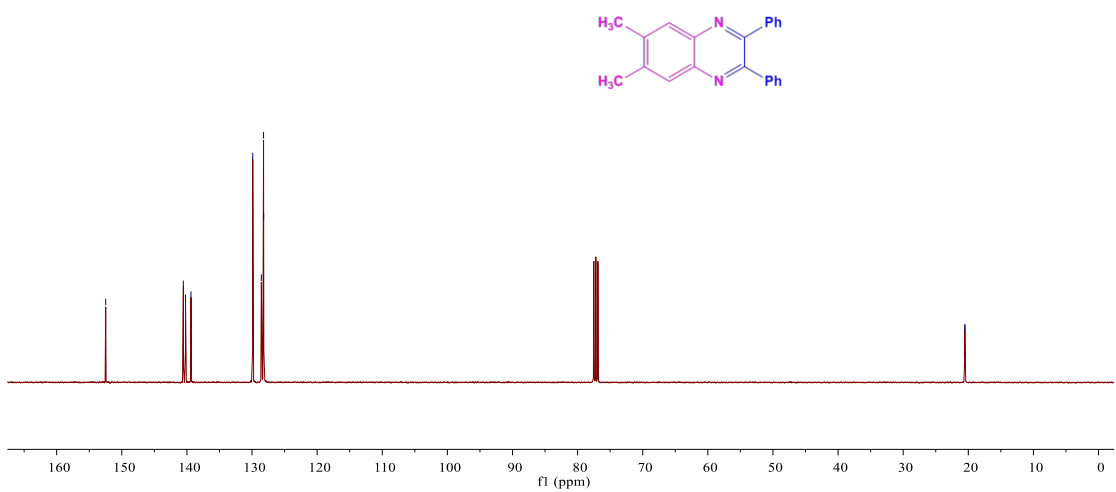
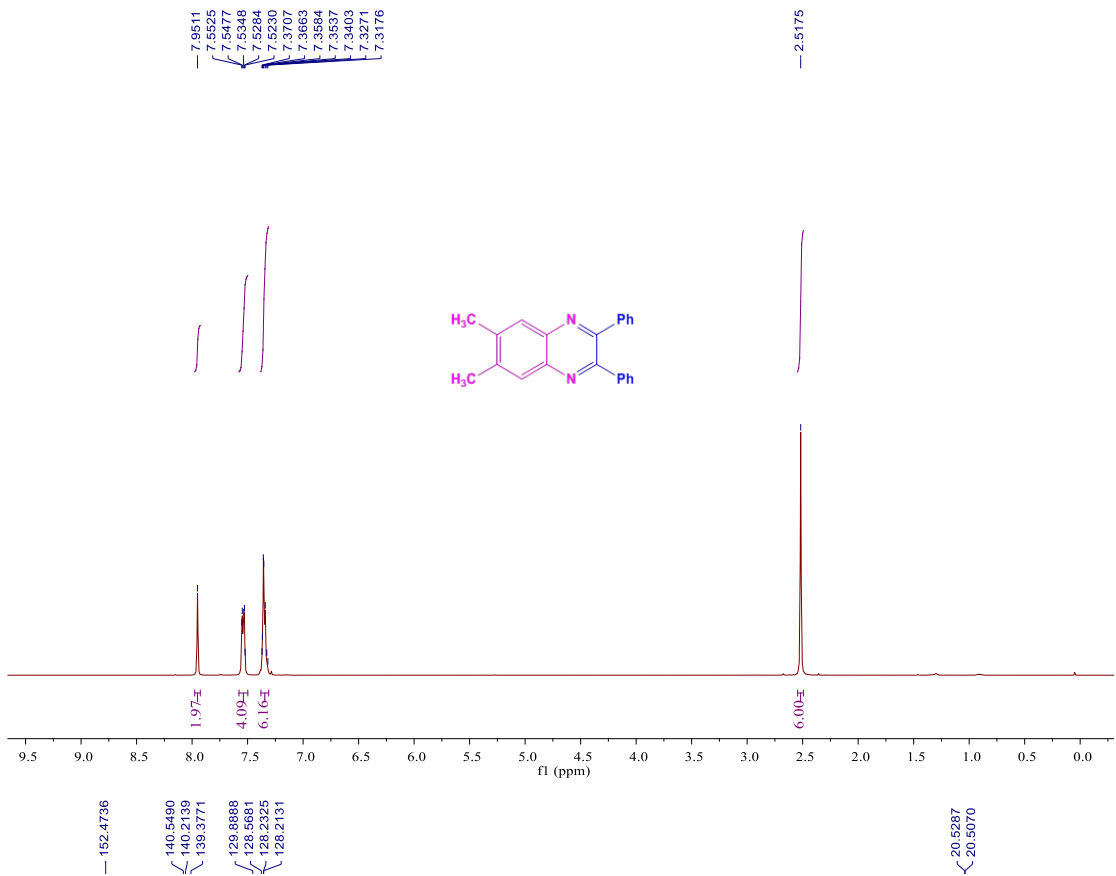


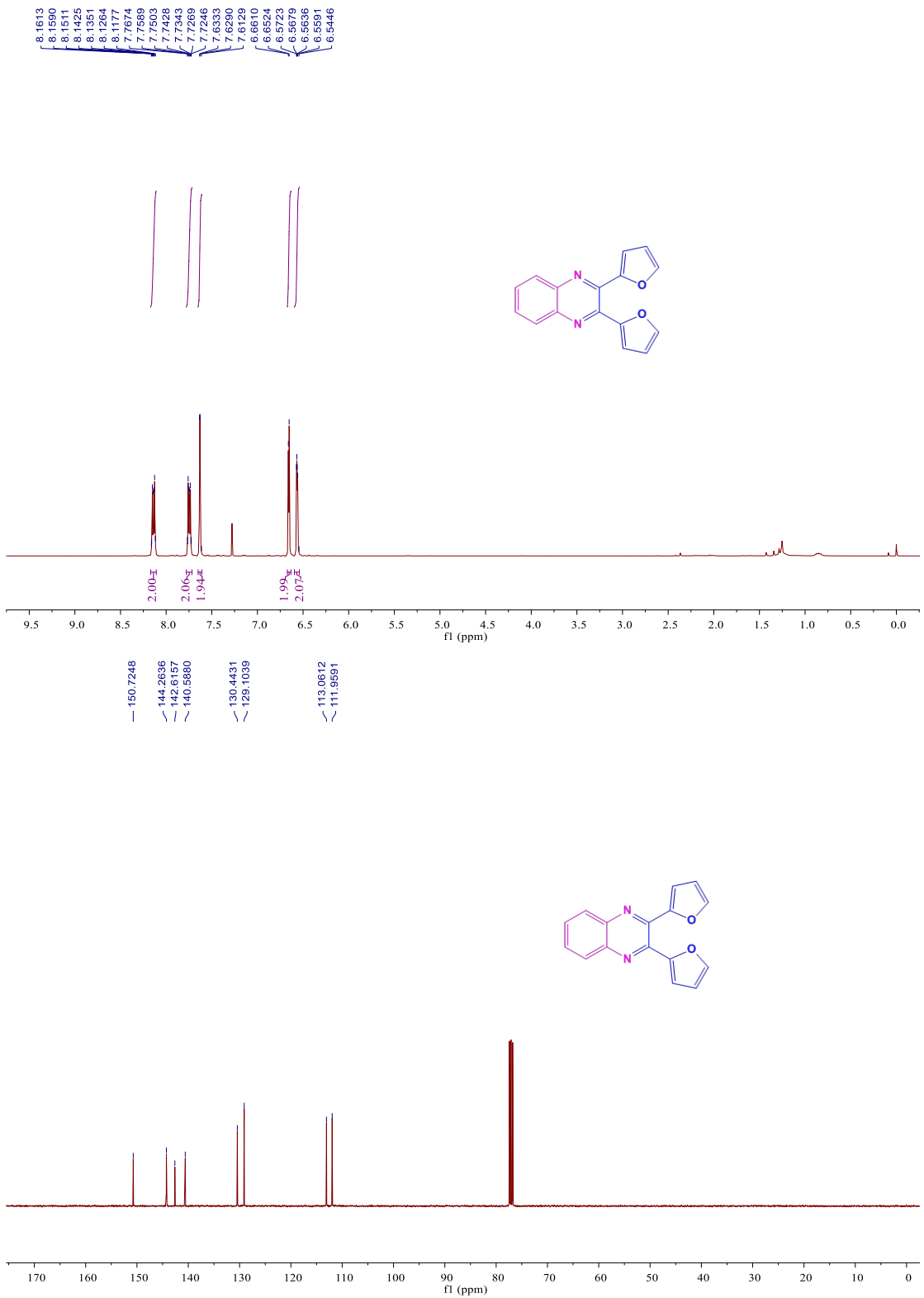


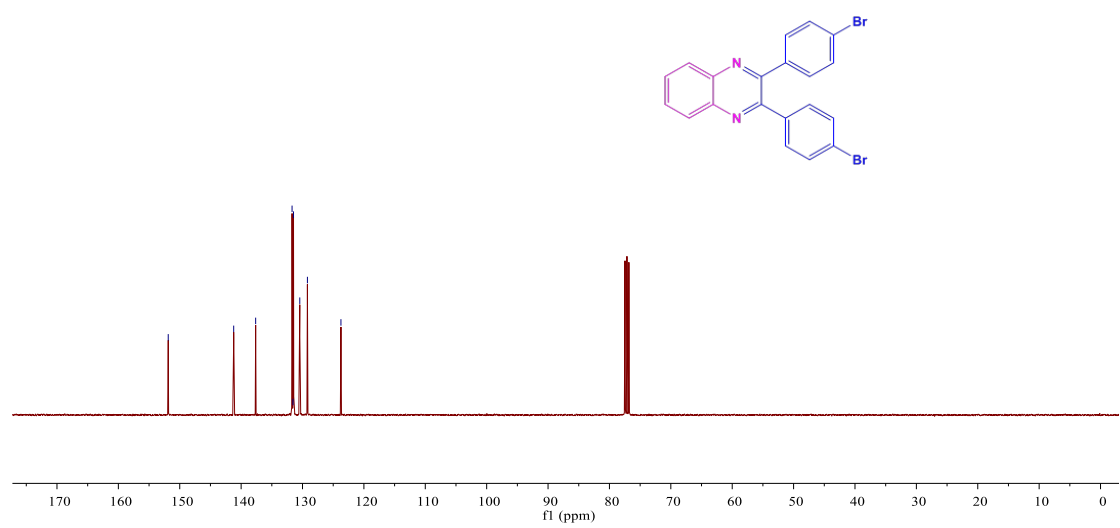
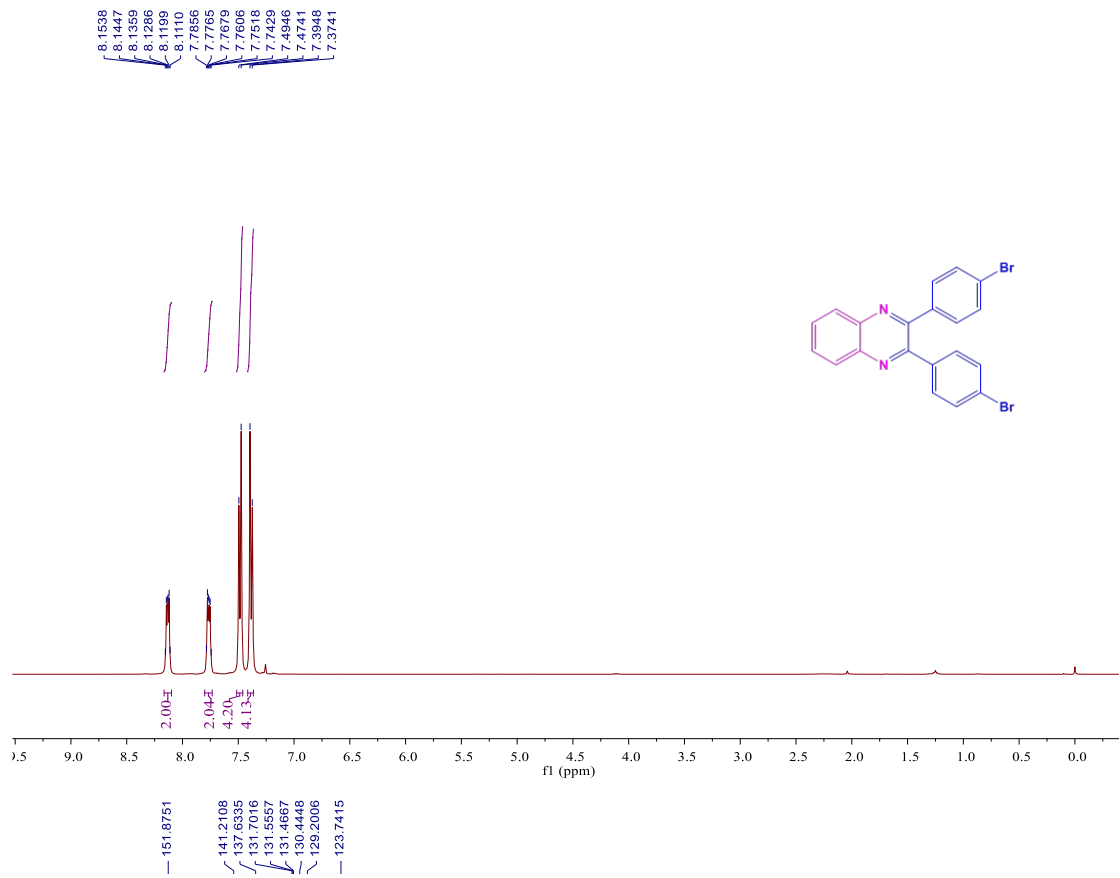
— 22.0224

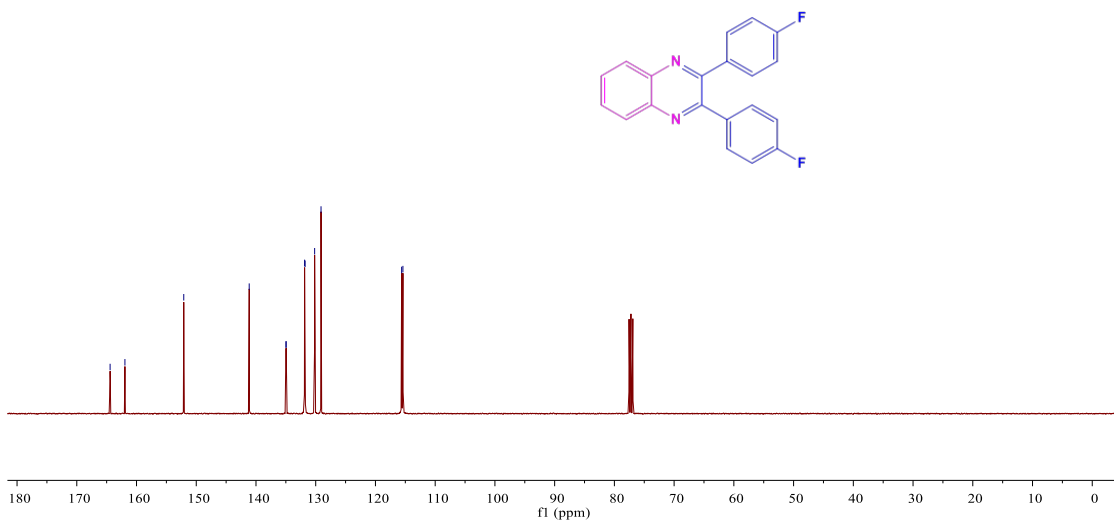
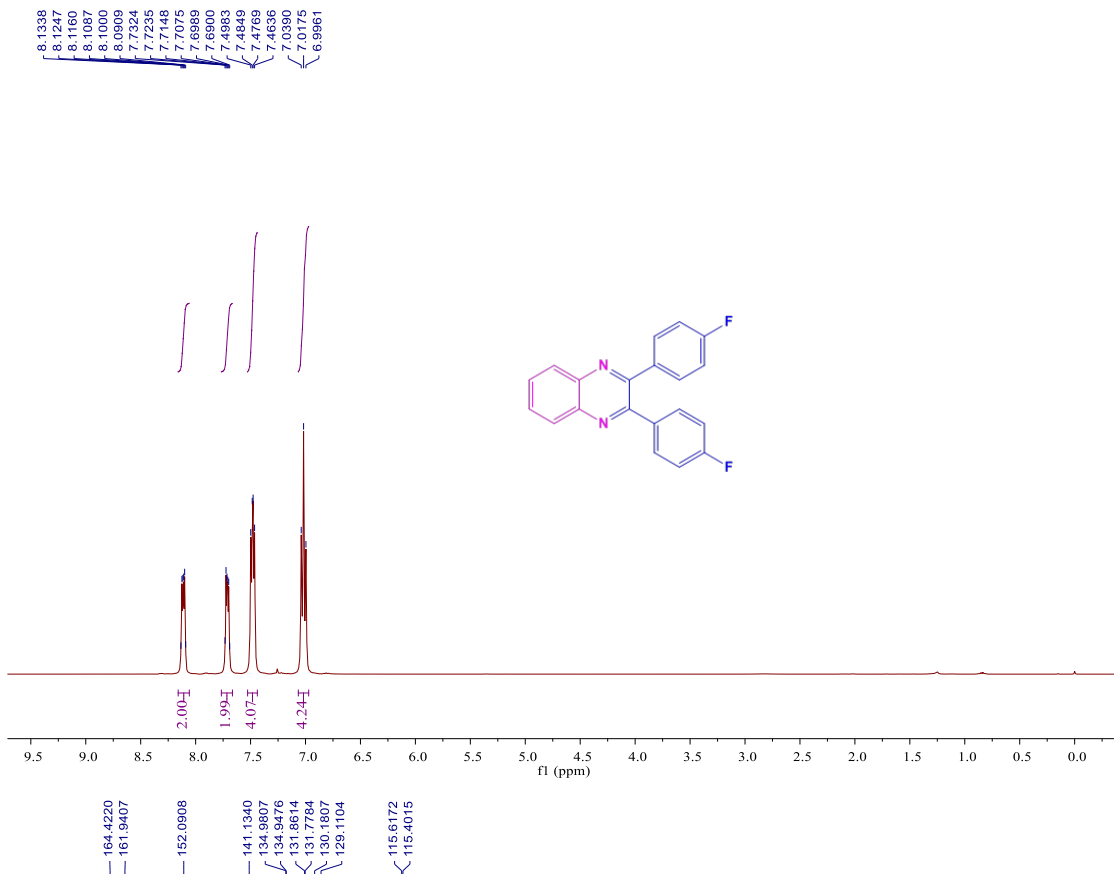








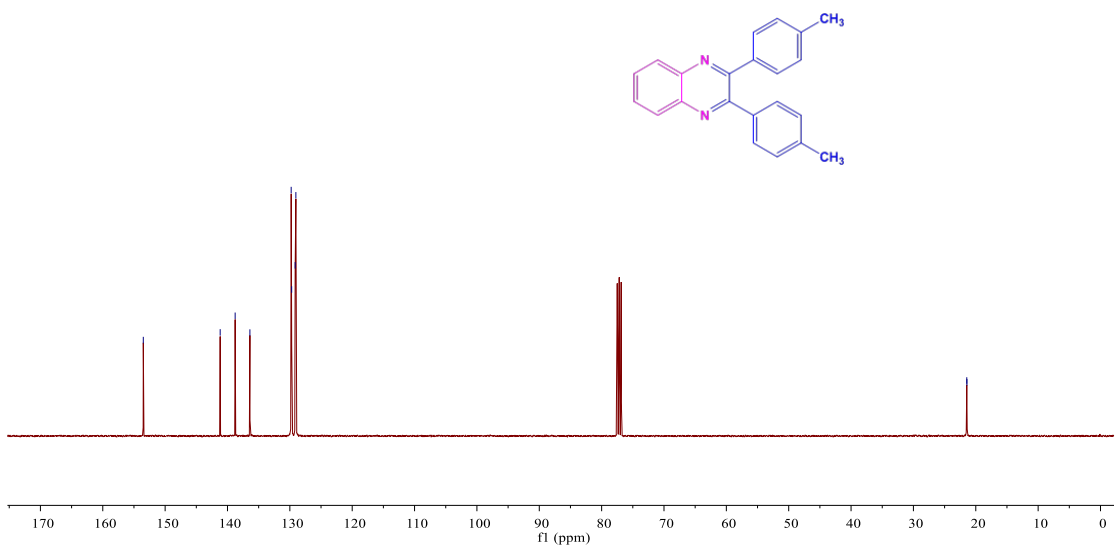


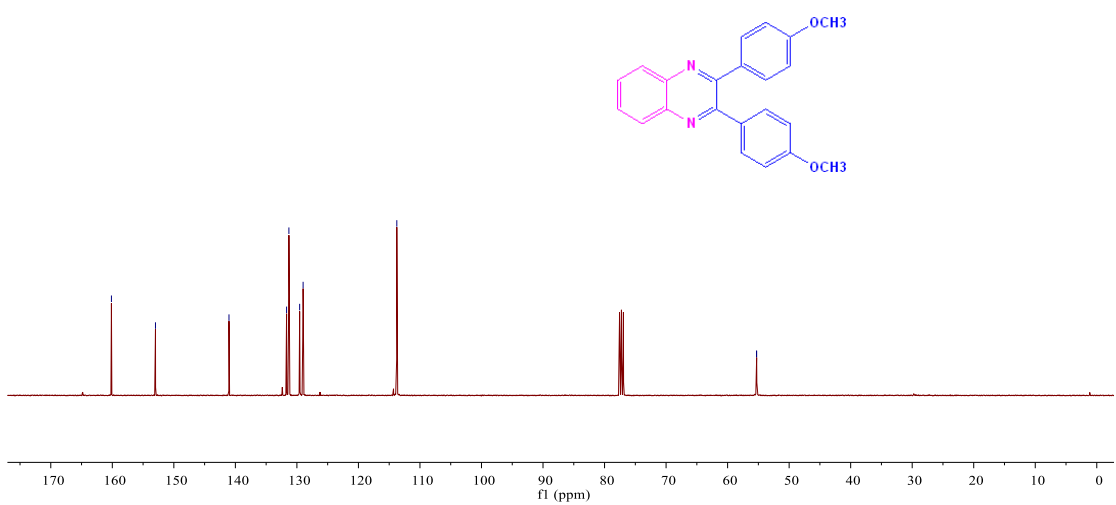
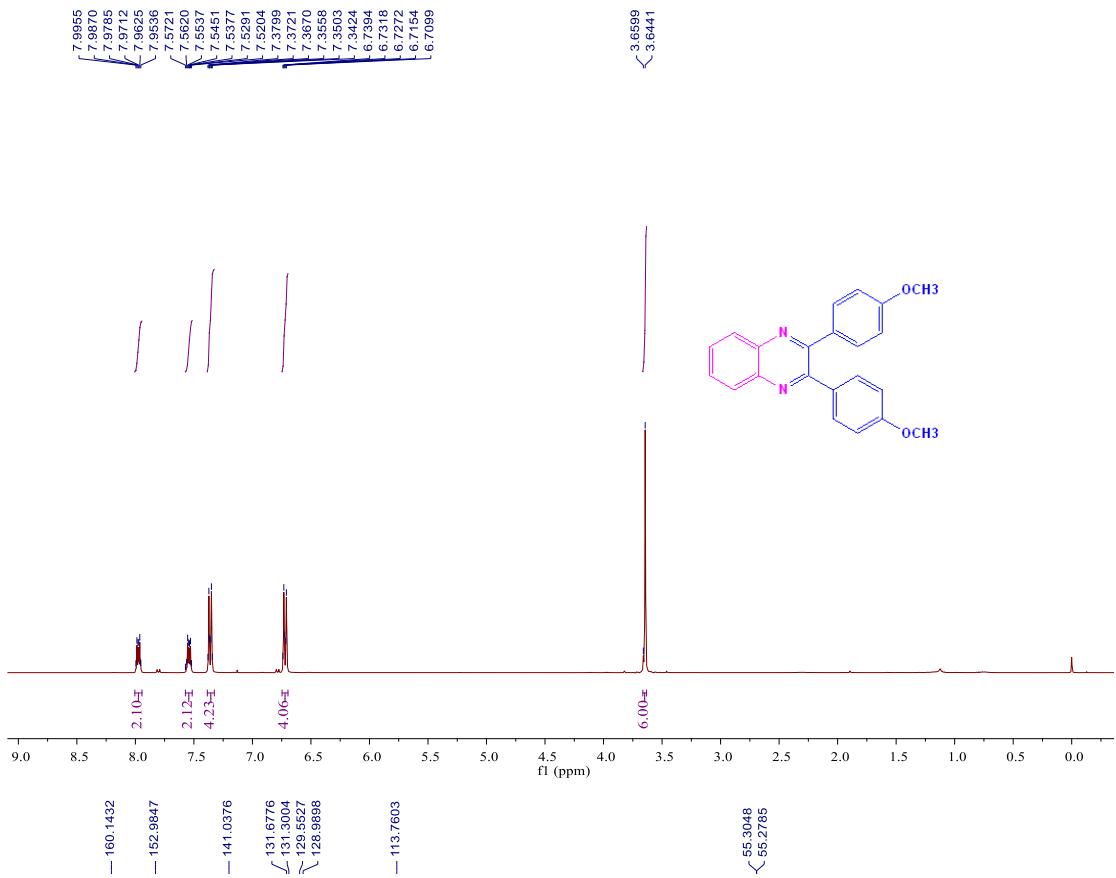


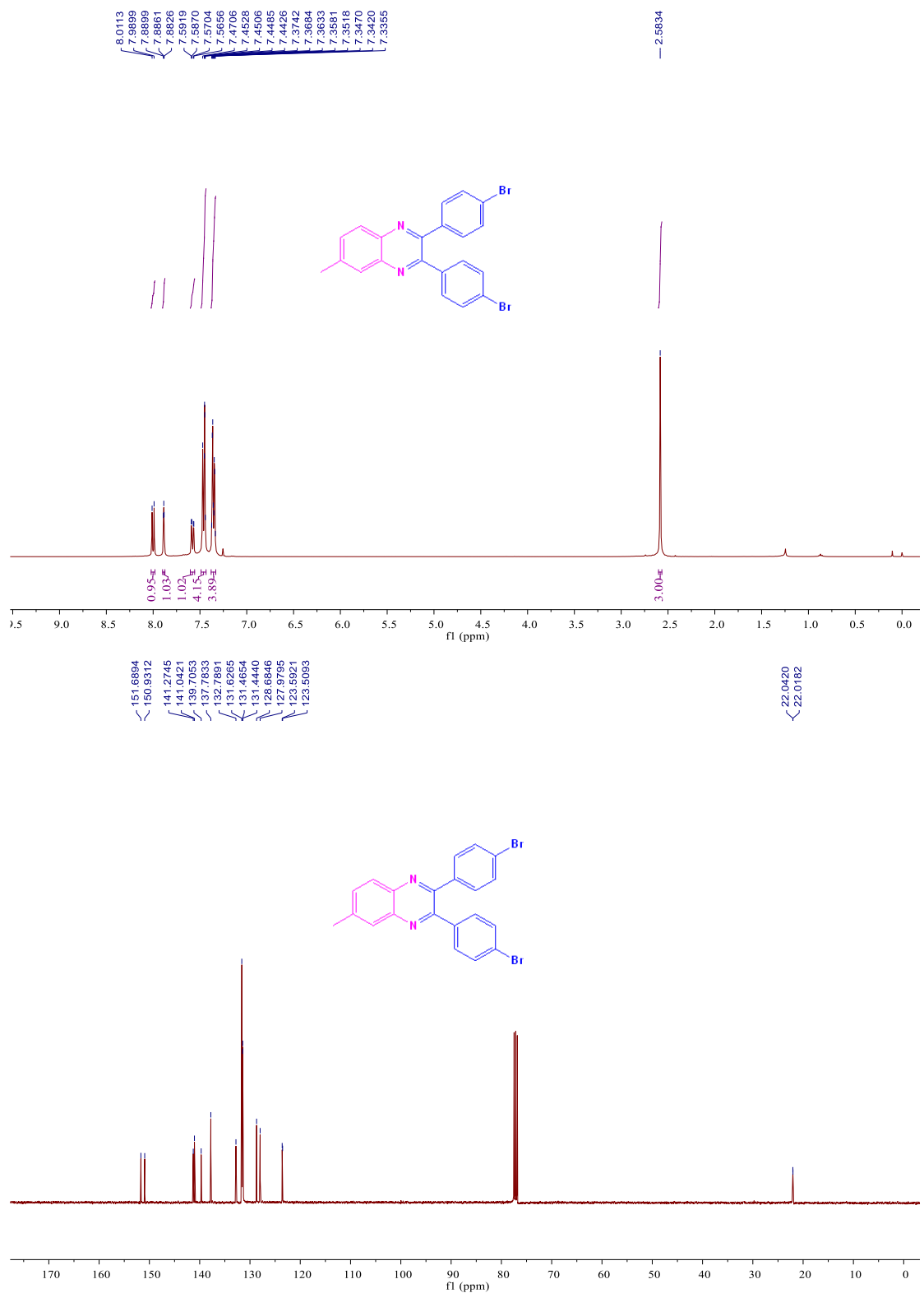


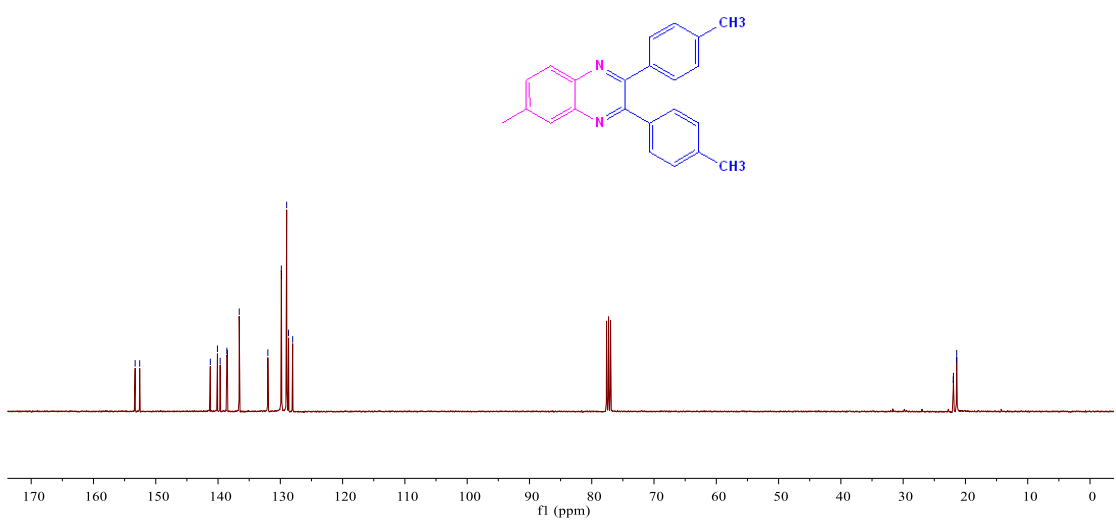
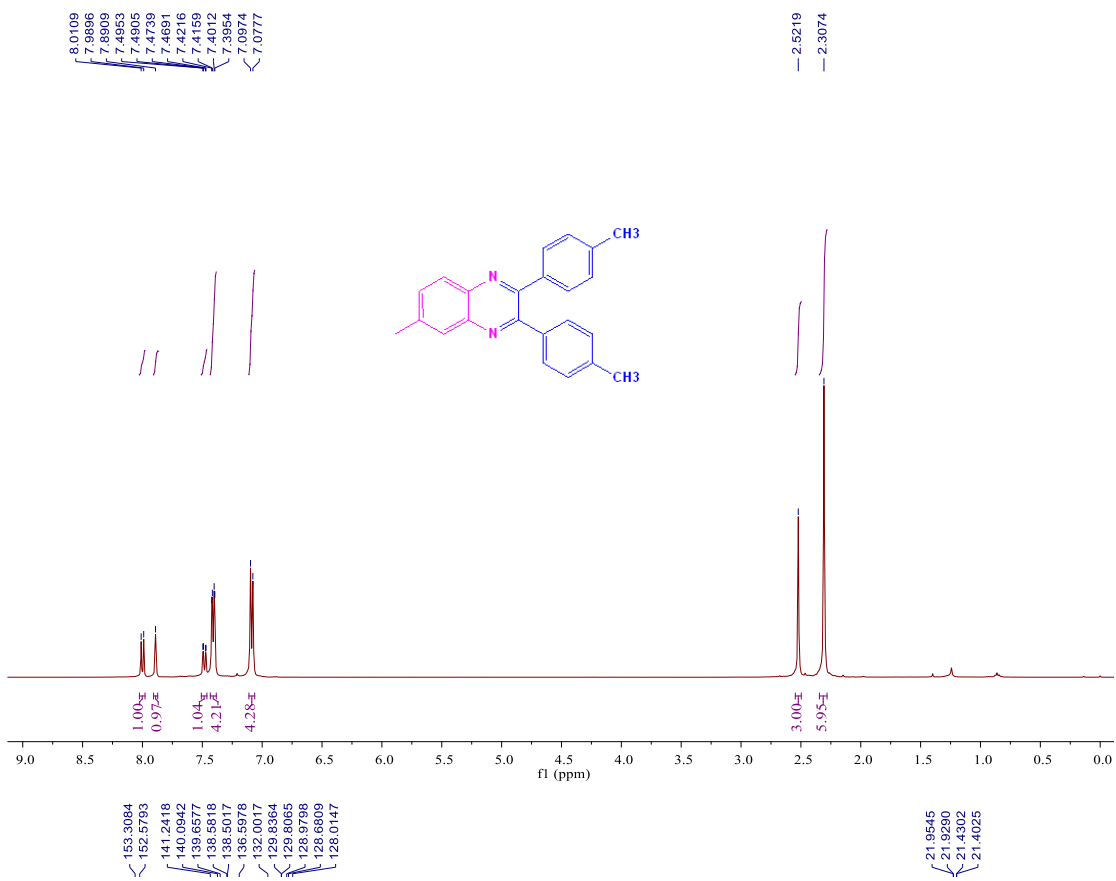
— 153.5010
 — 141.1723
 — 138.7712
 — 136.4066
 { 129.7974
 { 129.7091
 { 129.1463
 { 129.0347

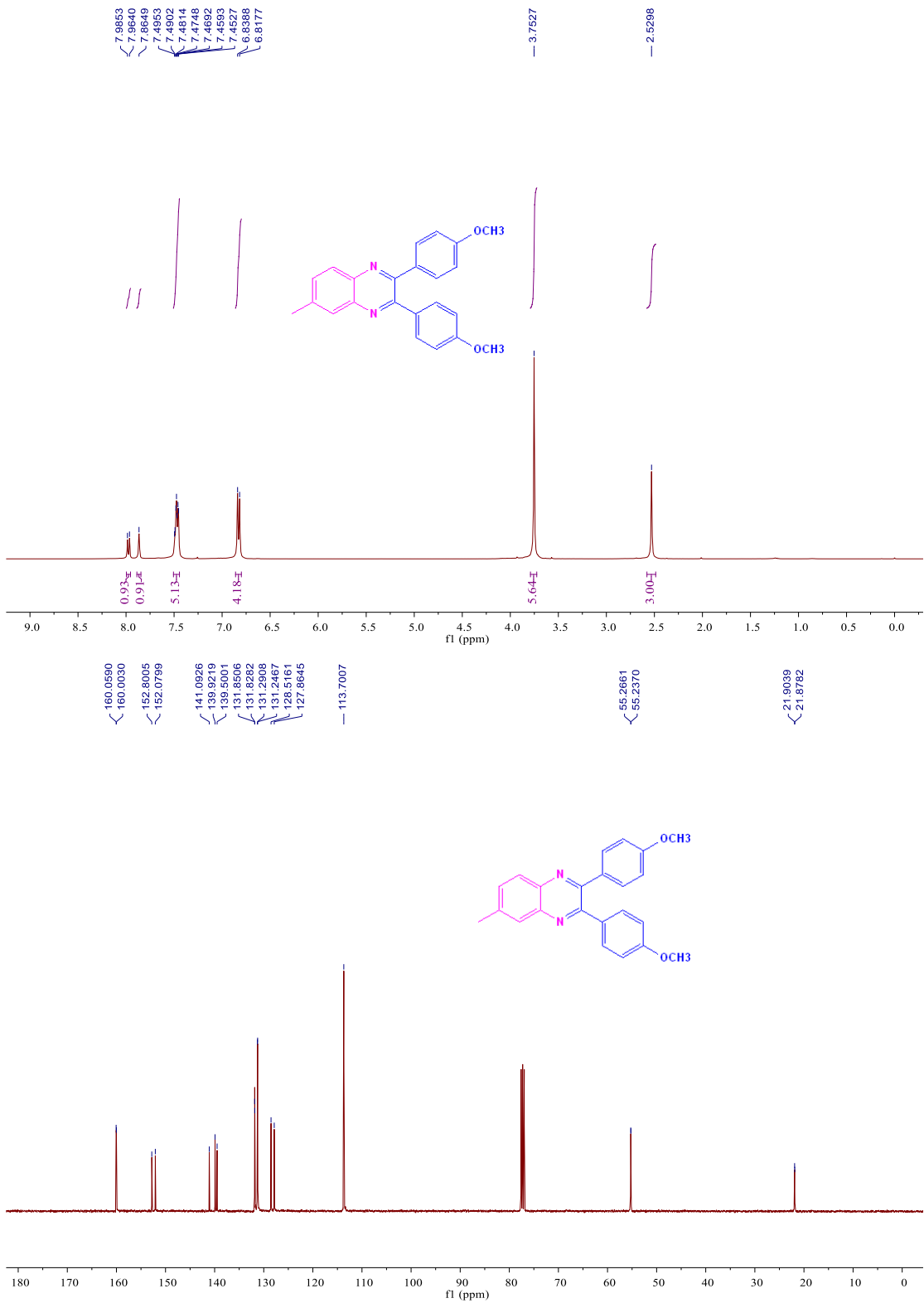
< 21.4440
 < 21.4224

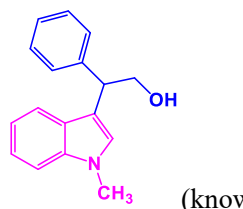




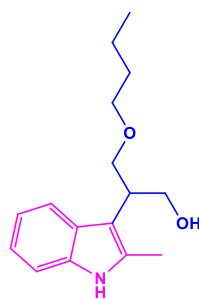
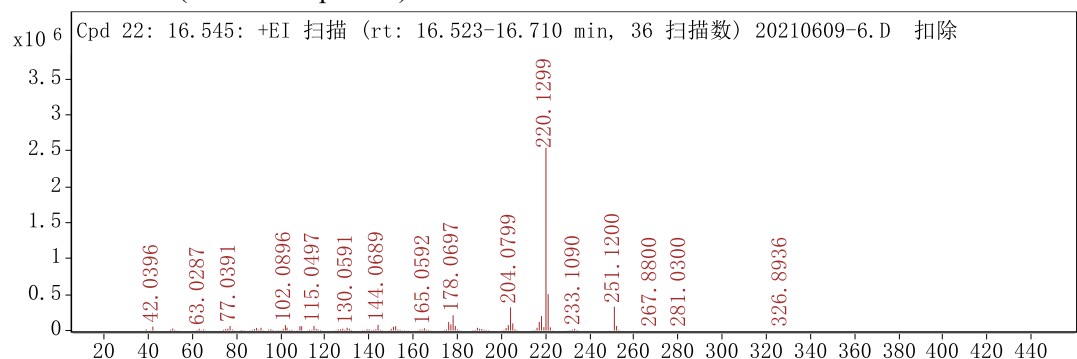




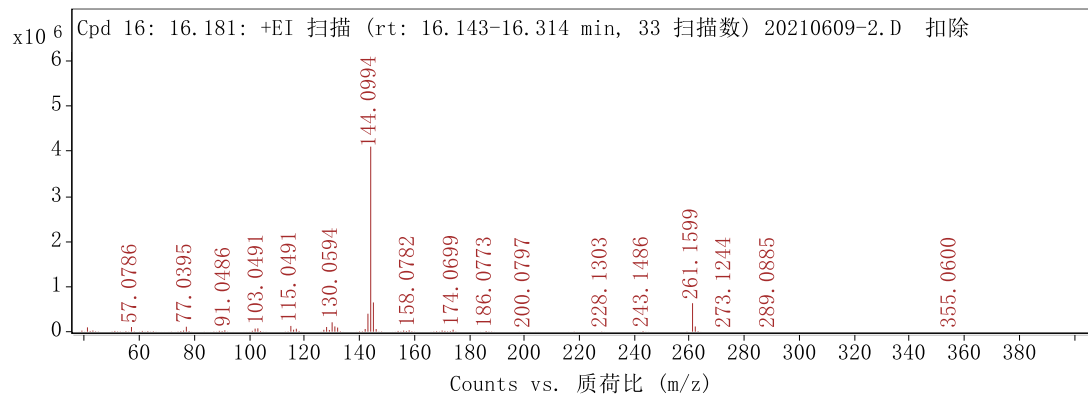


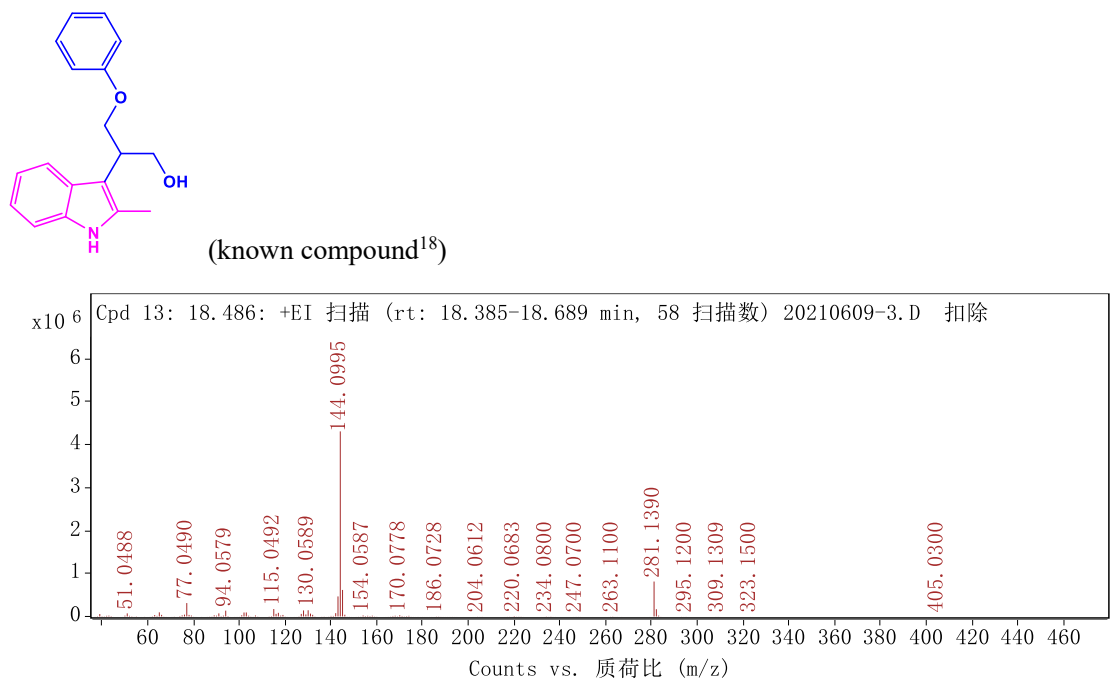


(known compound³)



(known compound¹⁷)





4. References

1. J. S. Yadav, B. V. Reddy, S. Abraham and G. Sabitha, *Synlett*, 2002, **9**, 1550-1552.
2. B. P. Bandgar and A. V. Patil, *Tetrahedron Letters*, 2007, **48**, 173-176.
3. N. Nagarjun, P. Concepcion and A. Dhakshinamoorthy, *Molecular Catalysis*, 2020, **482**, 110628.
4. M. M. Nasef, M. Zakeri, J. Asadi, E. Abouzari-Lotf, A. Ahmad and R. Malakooti, *Green Chemistry Letters and Reviews*, 2016, **9**, 76-84.
5. M. Zakeri, M. M. Nasef, E. Abouzari-Lotf and H. Haghi, *Research on Chemical Intermediates*, 2015, **41**, 10097-10108.
6. M. Hosseini-Sarvari and G. Parhizgar, *Green Chemistry Letters and Reviews*, 2012, **5**, 439-449.
7. R. Parella, Naveen and S. A. Babu, *Catalysis Communications*, 2012, **29**, 118-121.
8. M. Kantam, R. Chakravarti, B. Sreedhar and S. Bhargava, *Synlett*, 2008, **2008**, 1449-1454.
9. J. S. Yadav, B. V. S. Reddy and G. Parimala, *J Chem Res*, 2003, 78-81.
10. M. Karimi, T. Hajiashrafi, A. Heydari and A. Azhdari Tehrani, *Applied Organometallic Chemistry*, 2017, **31**, e3866.
11. C. Zhou, J. Lei, Y. Liu, C. T. Au, Y. Chen and S. F. Yin, *Applied Organometallic Chemistry*, 2020, **34**.
12. A. Sharma, R. Dixit, S. Sharma, S. Dutta, S. Yadav, B. Arora, M. B. Gawande and R. K. Sharma, *Molecular Catalysis*, 2021, **504**, 111454.
13. J. H. Hansen and V. Elumalai, *SynOpen*, 2021, **05**, 43-48.
14. M. Kumaresan, V. Saravanan, P. Sami and M. Swaminathan, *Research on Chemical Intermediates*, 2020, **46**, 4193-4209.
15. D. Kumar, K. Seth, D. N. Kommi, S. Bhagat and A. K. Chakraborti, *RSC Advances*, 2013, **3**, 15157.
16. P. S. Chandrachood, A. R. Jadhav, D. R. Garud, N. R. Deshpande, V. G. Puranik and R. V. Kashalkar, *Research on Chemical Intermediates*, 2020, **46**, 5219-5230.
17. E. Colacino, F. Delogu and T. Hanusa, *ACS Sustainable Chemistry & Engineering*, 2021, **9**, 10662-10663.
18. K. Tabatabaeian, M. Mamaghani, N. O. Mahmoodi and A. Khorshidi, *Tetrahedron Letters*, 2008, **49**, 1450-1454.